Melanie Janine Ballach, MSc

Examination of neovascularization and oxygenation of the subcutaneous adipose tissue after long-term implantation of continuous subcutaneous insulin infusion catheters

Master Thesis

submitted in fulfilment of the requirements for the degree of
graduate engineer (Diplom-Ingenieurin)
in Chemical and Pharmaceutical Engineering

at

Graz University of Technology

Supervisor
Univ.-Prof. Dr.rer.nat. Rudolf Bauer
Institute of Pharmaceutical Sciences
University of Graz

Co-Supervisor
Jasmin Hauzenberger, PhD
Clinical Department of Endocrinology and Diabetology
Medical University of Graz

2018

STATUTORY DECLARATION

I declare that I have authored this thesis independently, that I have not used other than the declared sources / resources, and that I have explicitly marked all material which has been quoted either literally or by content from the used sources. The uploaded text document at TUGRAZonline is identical with the present master thesis.

Date

Signature

EIDESSTATTLICHE ERKLÄRUNG

Ich erkläre an Eides statt, dass ich die vorliegende Arbeit selbstständig verfasst, andere als die angegebenen Quellen/Hilfsmittel nicht benutzt, und die den benutzten Quellen wörtlich und inhaltlich entnommenen Stellen als solche kenntlich gemacht habe. Das in TUGRAZonline hochgeladene Textdokument ist mit der vorliegenden Masterarbeit identisch.

Datum

Unterschrift

Acknowledgement

Hereby, I would like to thank everyone who supported and accompanied me during this thesis.

First, I would like to thank Prof. Dr. Rudolf Bauer and Jasmin Hauzenberger, PhD, who made this thesis possible for me.
A big thank you to Petra Kotzbeck and Julia Münzker for the commitment, support, advice and for taking time for discussions.
Thanks again to Jasmin Hauzenberger, PhD, for the supervision, support and the great constant help whether in the laboratory or in the analysis of data.
Additionally, I would like to thank Julia Brunner, BSc for her support in the laboratory.
Thank you as well to the PhD students from the Division of Endocrinology and Diabetology for the great and productive discussions, suggestions and for the acceptance in the group.
A big thank you to Melanie Brandner and Joseph Redden for correcting the grammar of my written English.

Finally, I would like to thank my family for their support at all levels. I would not have been able to conduct this master program without them. And lastly, thank you to my little daughter, Hannah Marie, who pushed me to finish this thesis as quickly as possible.

Abstract

Approximately 1 million patients with type 1 diabetes use continuous subcutaneous insulin infusion (CSII) systems. New approaches are in development where continuous glucose monitoring and insulin infusion are combined using one catheter. These single-port systems measure the glucose level continuously via an O_2-based sensor. Under hypoxic conditions, such as the acute inflammatory response to catheter insertion, this measurement may be compromised. To study the effect of insertion trauma on tissue oxygenation, an animal study was performed in 10 farm swine. Teflon and steel CSII catheters were inserted into the subcutaneous tissue and maintained for a maximum of 7 days. RNA was isolated from the tissue surrounding the catheters and seven genes related to hypoxia, angiogenesis or vascularization were investigated using real-time PCR.

Angiogenesis inducer TGF-β increased over wear-time around both materials, however, there was no effect on VEGF and CD31 within 7 days. Hypoxic conditions were observed by an increase in HIF-1α within 1 day. Wound healing factors MMP2 and FN increased over wear-time of both steel and Teflon catheters. Differences between tip and center were observed in some instances but in general, oxygen distribution was homogenic along the catheters.

In conclusion, the acute inflammatory response launches induction of angiogenesis but within 7 days, no formation of new vessels takes place. Tissue along catheters is homogeneously supplied with oxygen and irregular supply may not interfere with O_2-based glucose measurement. The data analyzed and discussed in this thesis can be considered for the development of optimized single-port catheter designs in the future.

Zusammenfassung

Etwa 1 Million Typ 1 Diabetiker verwenden kontinuierliche subkutane Insulininfusionssysteme (CSII). Es wird an neuen Ansätzen gearbeitet, bei denen kontinuierliches Glukosemonitoring mit Insulininfusion auf einem Katheter kombiniert werden. Diese sogenannten „Single-Port"-Systeme messen kontinuierlich den Glukosespiegel mithilfe eines O_2-basierten Sensors. Unter hypoxischen Bedingungen, wie der akuten Entzündungsantwort auf die Kathetereinführung, kann jedoch dieses Messsystem variable Ergebnisse liefern. Um die Auswirkung eines Insertionstraumas auf die Sauerstoffversorgung des Gewebes zu untersuchen, wurde eine Studie mit 10 Hausschweinen durchgeführt. Teflon- und Stahl-CSII-Katheter wurden in das subkutane Gewebe eingebracht und verblieben dort für maximal 7 Tage. RNA wurde aus dem die Katheter umgebenden Gewebe isoliert und sieben Gene, die mit Hypoxie, Angiogenese oder Vaskularisierung in Zusammenhang stehen, wurden mithilfe der quantitativen Echtzeit-PCR untersucht.

Der Angiogenese-Induktor TGF-β war während der Tragedauer um beide Materialien erhöht, jedoch gab es keine Auswirkung auf VEGF und CD31 innerhalb von 7 Tagen. Hypoxische Bedingungen wurden durch einen Anstieg von HIF-1α innerhalb eines Tages beobachtet, mit einer höheren Expression um den Stahlkatheter. Die Wundheilungsfaktoren MMP2 und FN waren während der Tragedauer von Stahl- und Teflonkathetern erhöht. Unterschiede zwischen Spitze und Mitte wurden in einigen Fällen beobachtet, aber im Allgemeinen war die Sauerstoffverteilung entlang der Katheter homogen.

Zusammenfassend lässt sich sagen, dass die akute Entzündungsreaktion die Induktion der Angiogenese auslöst, jedoch innerhalb von 7 Tagen findet keine Bildung neuer Gefäße statt. Das Gewebe entlang der Katheter wird homogen mit Sauerstoff versorgt und eine unregelmäßige Zufuhr kann die O_2-basierte Glukosemessung nicht stören. Die in dieser Arbeit analysierten und diskutierten Daten können zukünftig in der Entwicklung von optimierten Single-Port-Katheten berücksichtigt werden.

Contents

List of Figures

List of Tables

List of Equations

1. Introduction

The autoimmune disease type 1 diabetes occurs all over the world (Daneman 2006). People suffering from type 1 diabetes are dependent on frequent dosing of insulin to manage their blood glucose levels (Voet et al. 2002, Chiang et al. 2014). Insulin can be applied via a pen, a syringe, or continuous subcutaneous insulin infusion (CSII) (Daneman 2006, Shalitin and Phillip 2007). The most advanced therapy on the market today to improve life of the patient is the combination of a continuous glucose monitoring (CGM) and a CSII system that communicate with each other through an algorithm ("artificial pancreas") (Gifford 2013, Ang et al. 2015, Rodbard 2016). However, this form therapy is very expensive and so far, there is no fully-automated artificial pancreas (closed-loop) available (Ang et al. 2015, Rodbard 2016). Automating insulin delivery based on continuous glucose measurements is difficult due to inter- and intra-individual demands, depending on factors such as food intake and exercise (Ang et al. 2015). Furthermore, when a foreign body (cannula, sensor, etc.) is inserted into the subcutaneous adipose tissue, it elicits an inflammatory response that may influence the performance of an artificial pancreas system (Gifford 2013). The introduction of foreign material causes an acute trauma leading to the activation of the immune system. This acute inflammatory response may not only influence the absorption of insulin into the vasculature (Hauzenberger et al. 2017), but also the performance of an O_2-based glucose sensor (Gifford 2013). This thesis focusses on studying the changes in neovascularization and oxygenation of the subcutaneous adipose tissue over the wear-time of a CSII catheter.

1.1 Type 1 diabetes

Type 1 diabetes (formerly "juvenile diabetes") is an autoimmune disease which mostly develops in early childhood and is the most common chronic disease in children under the age of 18 years (Chiang et al. 2014, Krzewska and Ben-Skowronek 2016). The incidence of this disease varies from country to country. While in China and Venezuela rates are low, Finland and Sardinia exhibit the highest rates (Soltesz et al. 2007). Since 1998, the number of patients with diabetes has increased around 40 % in Central Europe. In Austria 30,000 people (thereof approximately 3,000 children) are suffering from diabetes type 1 (Österreichische Diabetes Gesellschaft: http://www.facediabetes.at/zahlen-und-fakten.html). So far there is no holistic cure for this disease and patients are dependent on the application of insulin.

Type 1 diabetes leads to high blood glucose levels, which are caused by a deficiency of the hormone insulin due to the destruction of insulin producing beta cells of the pancreas by endogenous antibodies (Daneman 2006, Todd 2010, Silbernagl and Lang 2013, Chiang et al. 2014, Phillips 2016). Insulin is essential for the body as it is responsible for glucose uptake into muscle and fat cells (Silbernagl and Lang 2013). If insulin producing beta cells are destroyed by endogenous antibodies, certain transporters in the body cannot be opened and glucose uptake from the blood is impossible. Therefore, the blood glucose level increases which can lead to hyperglycemia and consequently to clinical complications such as diabetic ketoacidosis (Voet et al. 2002, Trachtenbarg 2005, Phillips 2016). The body requires glucose as an energy source for cells and organs. If there is a lack of insulin, cells and organs will starve (Voet et al. 2002, Colditz et al. 2005). Alternatively, the body can cover its energy demands via an elevated secretion of glucagon, catecholamines (e.g. norepinephrine) and glucocorticoids (e.g. cortisol), which leads to an increase in β-oxidation, gluconeogenesis and ketone bodies (by-product of β-oxidation). The degradation of fats/fatty acids and the production of ketone bodies (weak acids) lowers the pH (acidosis) of the blood. This is called diabetic ketoacidosis (Voet et al. 2002, Colditz et al. 2005, Trachtenbarg 2005, Silbernagl and Lang 2013).

1.2 Continuous subcutaneous insulin infusion (CSII) systems

There are various forms of insulin application with the main goal of strictly controlling blood sugar levels. This can be achieved either via a pen, a syringe or insulin pumps (CSII systems) (Daneman 2006, Shalitin and Phillip 2007).

CSII systems consist of a pump body and an insulin infusion set. This insulin infusion set is necessary to deliver insulin from the pump reservoir via the tubing into the body (Pickup and Keen 2002, Heinemann 2016). The infusion of insulin into the subcutaneous adipose tissue occurs either via a Teflon or steel cannula. The Teflon cannula requires a steel guiding needle to be accurately inserted into the skin, which can be removed afterwards, whereas the steel cannula remains in the skin for the duration of the therapy (Heinemann 2016).

Basically, in CSII therapy short-acting insulin is continuously delivered into the body to cover the basic requirement (basal rate). This basal rate is interrupted by a bolus (a larger quantity of insulin) to account for meal carbohydrates (Pickup and Keen 2002, Heinemann et al. 2014).

In general, CSII catheters can be used for approximately 2 to 3 days before they need to be replaced. The main reason for replacing an infusion set is the increase in insulin absorption variability over wear-time. Some patients use the infusion set more than 3 days without any skin reaction or other adverse events, while others need to change it daily (Patel et al. 2014, Heinemann 2016). Additionally, the risk of occlusion increases with increasing duration of wear-time. Another disadvantage is the possibility of the formation of air bubbles in the insulin solution due to higher temperatures for example. This may lead to insufficient insulin doses resulting in, for example, hyperglycemia (Heinemann 2016).

Advantages of the CSII are improved glycemic control and therefore, quality of life (Weissberg-Benchell et al. 2003). Nonetheless, insulin pump therapy with all its benefits is not applicable for everyone. Patients using insulin pump therapy need to fulfill certain prerequisites like willingness and ability to learn about pump therapy, monitor blood glucose regularly on their own, no psychiatric disorder, etc. (Sikes and Weyman 2017).

Lastly, insulin pumps are expensive and certain educational facilities for the medical team to introduce and supervise patients using those pumps are necessary (Pickup and Keen 2002).

In this thesis, two different cannula materials are inserted into the porcine skin to examine the effect of catheter insertion and maintenance on neovascularization and oxygenation. The cannulas for insulin infusion consist of either steel or Teflon, both 6 mm in length and 0.33 or 0.50 mm in external diameter, respectively. There are limited scientific publications available about the characteristics and distribution of the use of steel and Teflon cannulas. There are also no guidelines for insulin pump application available, which clearly recommend one of the two materials (Heinemann 2016). The choice of the material used is based on personal preferences, opinions or experiences. The opinion of the attending physician as well as what covers the insurance in the respective country are additional factors (Facchinetti et al. 2013, Heinemann et al. 2014, Heinemann 2016, Rodbard 2016). In Germany around 40 % and in Europe around 25 % use steel cannulas, whereas in the United States only 10 % based on survey data. Explanations are the differences in metabolic control depending on the cannula material used. Steel, compared to Teflon, is not a flexible material and does not kink, which ensures a continuous flow into the body (Heinemann 2016). Additionally, another pro-argument of patients to use steel cannulas is the simple and easy insertion into the body and that there is no difference in the comfort of wearing steel or Teflon. In contrast to steel, Teflon

cannulas are commonly inserted with auto-insertion devices and due to the flexible material, the cannula often kinks (Heinemann et al. 2014).

1.3 The Artificial Pancreas (AP)

The artificial pancreas (AP) is a medical device for people suffering from diabetes mellitus. It consists of a sensor, which continuously measures the glucose level in the body, a pump for controlled insulin delivery and a computer. The AP evaluates the data obtained from the sensor and controls the pump by means of an algorithm for simulating the glucose-insulin regulatory circuit (Cobelli et al. 2011; Robert, 2013).

The AP continuously measures the blood glucose level and provides the body with an appropriate amount of insulin. It simulates the function of the β-cells located in the pancreas, which produce and release insulin. The AP is more useful compared to conventional insulin therapies or insulin pumps as it simulates the natural release of insulin. Closed-loop artificial pancreas, bionic pancreas and implanted artificial pancreas are the three main artificial pancreas systems (Diabetes.co.uk 2017).

For AP systems currently available, two separate devices are necessary: one to measure the glucose level and one to deliver insulin. Handling two devices might be difficult for some people. New approaches, where continuous glucose monitoring (CGM) and insulin infusion are combined on one catheter have recently been proposed (Lindpointner et al. 2010, Lindpointner et al. 2010 (1), Hajnsek et al. 2014, Rumpler et al. 2017). This offers an improvement in patients' diabetes treatment. Furthermore, such a single-port system is advantageous as there is only one insertion necessary. It is thus once associated with pain and a risk of infection (Rumpler et al. 2017).

A single-port system has two different units. The sensor unit consists of a glucose sensor and a reference oxygen sensor based on phosphorescence, which are coated onto the cannula of the insulin infusion set (Rumpler et al. 2017). In a proof-of-concept trial, the coating of the cannula consisted of two layers. One layer contained the enzyme glucose oxidase (GOx), which acts as glucose-specific receptor. GOx catalyzes the conversion of glucose and oxygen to gluconolactone and hydrogen peroxide. The other layer had a luminescent dye which is sensitive to oxygen (absorption and emission maxima at 617 nm and 768 nm) and was directly coated onto the cannula (Hajnsek et al. 2014). Rumpler et al. improved the glucose sensor with a third layer, a diffusion layer. Oxygen molecules can pass this outermost layer, while the diffusion of glucose molecules from the subcutaneous adipose tissue to the second layer (GOx) is limited. The other part of

the sensor unit is the reference oxygen sensor consisting of an oxygen-sensitive layer. This reference sensor is coated in proximity to the glucose sensor (2 mm distance). To avoid optical crosstalk between the two sensors, excitation and emission spectra of the two oxygen-sensitive layers are different. The optical read-out unit is placed above the sensors outside the body, which is able to read out the sensors and represent the second unit of the single-port system (Rumpler et al. 2017). A schematic diagram of a single-port system is shown in Figure 1.

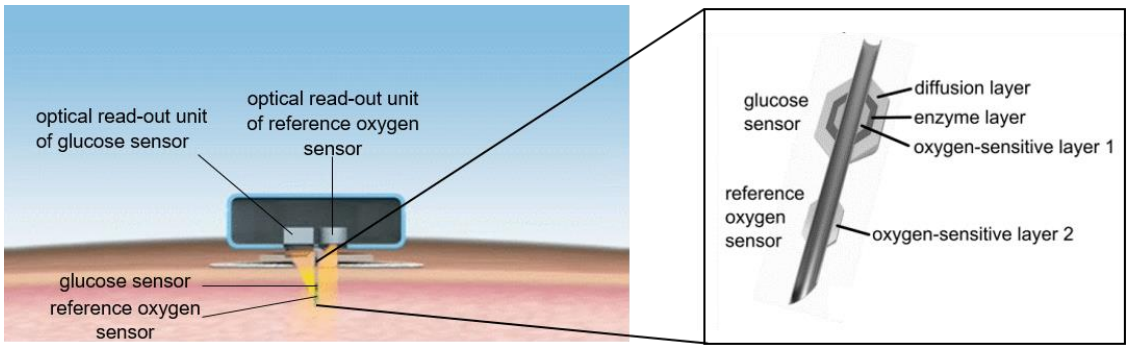

Figure 1: Schematic diagram of a single port system: The left image represents the single-port system with its sensor and optical read-out unit. The sensor unit consists of the two phosphorescence based oxygen sensors which are coated onto the cannula of an insulin infusion set. The read-out unit is responsible for read-out of the sensors and is placed above the sensors outside the body. This image was taken from Joanneum Research Forschungsgesellschaft mbH 2012 and independently labeled. The right image is a magnification of the sensors and their layers, which are coated onto the cannula of an insulin infusion set. This image was taken from Rumpler et al. 2017.

The single-port system is still being (pre-)clinically tested and not yet commercially available (Regittnig et al. 2013, Hajnsek et al. 2014, Tschaikner et al. 2015, Rumpler et al. 2017). There are various types of glucose sensors, for example electrochemical or O_2-based sensors. The glucose measurements with electrochemical sensors can be interfered by electrochemically active agents. In contrast to electrochemical sensors, optical glucose sensors based on oxygen sensors are not affected (Gifford 2013, Rumpler et al. 2017). Every sensor has its advantages and disadvantages. This thesis, however, only focusses on O_2-based CGM systems, where glucose is enzymatically (GOx) measured. As there is limited scientific expertise available, it is of interest to investigate the oxygen availability in the subcutaneous adipose tissue along the catheter. In the single-port system the two sensors are coated onto the cannula close to each other but still at a certain distance. For its functionality it would be a prerequisite that the oxygen availability does not change along the catheter.

1.4 The immune response to insulin infusion catheters

When a CSII catheter is introduced into the adipose tissue, the tissue is injured (disrupted capillaries, lymph vessels and connective tissue). This triggers a series of complex events causing the tissue healing response. These events include, among others, inflammation, wound healing and formation of granulation tissue. All of these complex events are necessary to maintain homeostasis (Anderson 2004, Ratner and Bryant 2004, Anderson et al. 2008).

After the cannula is inserted into the subcutaneous adipose tissue, the injured area is immediately flooded with blood and exudation occurs, where proteins and blood cells from the vascular system accumulate at the site of injury (Anderson 2001, 2004, Ratner and Bryant 2004). On the one hand, fibrin is activated from the inactive precursor fibrinogen within the blood. It is a fibrous protein that is responsible for blood clot formation as well as adhesion of platelets and aggregation to the fibrin plug. On the other hand, a provisional matrix with fibrin as the major component will be formed at the injury site, which happens within minutes to hours after the catheter is inserted into the tissue (Tonnesen et al. 2000, Anderson 2001, 2004, Ratner and Bryant 2004, Anderson et al. 2008). The provisional matrix releases components (structural and biochemical) which are necessary for the process of wound healing (Anderson 2004). Cytokines and growth factors (fibronectin, transforming growth factor β, platelet-derived growth factor) are such components and are responsible for the recruitment of white blood cells like neutrophils. Neutrophils are the predominant cells in the first few days of inflammatory reaction. Later, neutrophils are replaced by monocytes which differentiate into macrophages at the wound site. As they are long-living, they are present for days to weeks. The white blood cells – neutrophils, monocytes, macrophages – are important to clean the injury site. The wound site may contain bacteria and dead cells which are phagocytized (Anderson 2001, 2004, Ratner and Bryant 2004). Macrophages release reactive oxygen species (ROS) and matrix metalloproteinases (MMPs) that destroy bacteria and foreign material (Anderson et al. 2008, Seaton et al. 2015). Additionally, white blood cells recruit other cells which will convert the fibrin clot into vascularized granulation tissue containing fibronectin and hyaluronan (Tonnesen et al. 2000). The healing of the wound is associated with the formation of granulation tissue and proliferation of blood vessels and fibroblasts. Blood vessels are generated in a process called neovascularization or angiogenesis (Anderson 2001, 2004). Some fibroblasts differentiate into myofibroblasts that have smooth muscle cell characteristics which are responsible for wound contraction and moreover, the provisional wound matrix will be replaced by a mature scar matrix (Anderson 2001, 2004, Ratner and Bryant 2004).

The inserted biomaterial cannot be phagocytized by the adhered macrophages as this foreign body is much larger in size compared to these cells, they start fusing together to build foreign body giant (FBG) cells (Anderson 2001, Ratner and Bryant 2004, Anderson et al. 2008). If the foreign body possesses a flat and smooth surface, only a thin layer of macrophages will accumulate at the surface of the foreign body, whereas a thicker layer of macrophages and FBG cells will be at rough surfaces. Walling off of the inserted catheter is the final step of the foreign body response (FBR) (Anderson 2001). The entire process of the FBR occurs during the first two to four weeks after insertion of the catheter (Anderson et al. 2008, Sides and Stenken 2014).
The timeline of the immune response to the inserted biomaterial is shown in Figure 2.

Every eukaryotic cell requires energy for self-repair, maintaining tissue- and/or organ-specific functions and many more. All these processes are coupled to ATP hydrolysis, in which free energy is released. Oxidative phosphorylation is the process used from most of the cells, where metabolic substrate oxidation is coupled to ATP synthesis. This process takes place in the mitochondria and consumes oxygen proportional to the rate of ATP utilization, which means the higher the metabolic activity the higher the rate of the used oxygen (Guzy and Schumacker 2006). After catheter insertion, the immune response will be activated and immune cells arrive at the site of injury to fulfill their specific functions, which consumes oxygen. Oxygen availability in the tissue decreases. Adaptive processes will be activated if oxygen availability becomes limiting. Under hypoxic conditions the electron transport chain of mitochondria acts, for example, as an O_2-sensor and releases ROS. On the one hand, the ROS released triggers functional responses such as hypoxia-inducible factor-α and on the other hand, phagocytes release ROS to destroy bacteria and foreign material at the wound site (Gutteridge 1994, Guzy and Schumacker 2006, Seaton et al. 2015, Zeitouni et al. 2016).

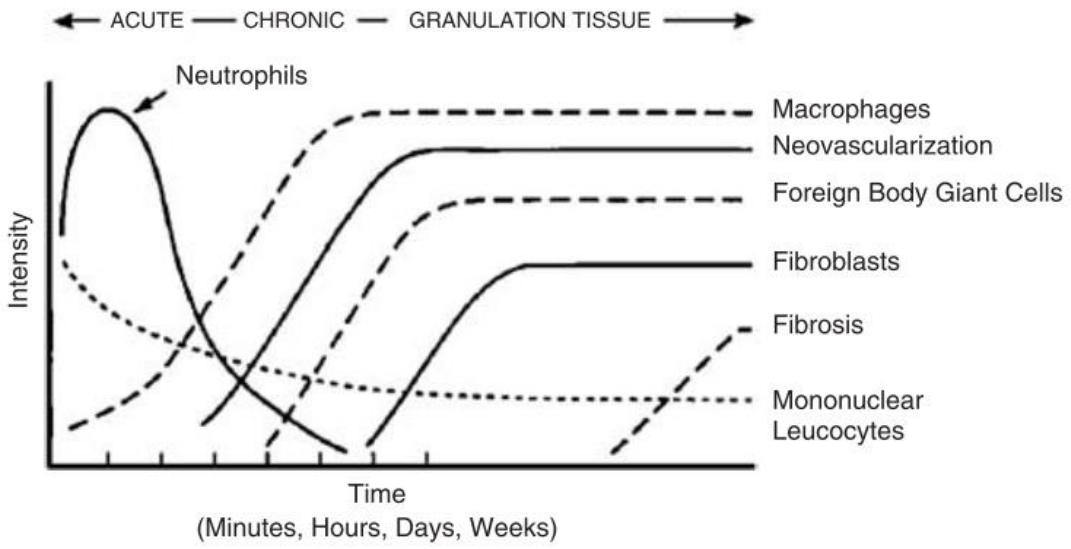

Figure 2: Immune response: Acute/chronic inflammatory response, development of granulation tissue and foreign-body reaction to biomaterials. The extent of the injury due to the biomaterial and its properties (size, shape etc.) is dependent on intensity as well as time. The graph was taken from Anderson, 2004.

Device failure, loss of functionality and other complications are important aspects and common considerations in manufacturing such insulin infusion catheters, which occur due to interface interactions or interactions between the foreign body and the host tissue and vice versa (Schoen 2004, Morais et al. 2010).

These hurdles are still present, and need to be overcome to provide patients with type 1 diabetes a better quality of life. So far, there is not enough knowledge to improve, cover or mask the foreign material in a way that the immune response will not be activated, when it enters the body. The immune response may be responsible for variable insulin absorption, which is why patients must change the insulin infusion catheter every 2 to 3 days to ensure an accurate supply of insulin from the subcutaneous adipose tissue (Hauzenberger et al. 2017). Furthermore, the acute inflammatory response to catheters may have a substantial impact on the performance of O_2-based glucose sensors which further needs to be elucidated.

1.5 The swine as an *in-vivo* model

Conducting research on wound healing on human skin is difficult. In order to obtain reproducible results there must be a sufficiently high number of humans with (nearly) identical wounds. The wound healing process needs to be examined and analyzed frequently, which is usually done via a histological assessment (Sullivan et al. 2001). Biopsies are taken and analyzed, which are painful and further infections and substantial

scarring may occur (Seaton et al. 2015). Hence, a human model for wound healing is not really feasible. For that reason, animal models with similar morphological and functional skin properties are used. Animal models should be selected carefully and many factors taken into account. In rodents, for example, the healing response is similar to human, except that deposited collagen leads to scar formation. The rodent model is cheap, small in size and easy to handle and to house. However, human wound healing differs from rodent wound healing in that, for example, rodent wound healing does not develop intra-abdominal adhesions (Wang et al. 2001). In addition, rodent models close their wounds primarily through wound contraction (Seaton et al. 2015), whereas humans through reepithelialization (Sullivan et al. 2001). Moreover, a large number of rodents would be necessary to achieve the same results as in swine due to the size of the excised tissue (Wang et al. 2001, Seaton et al. 2015). There are also other factors for choosing an animal model, such as availability and investigator familiarity.

The domestic swine provides the best alternative model to a human for experimental skin research (Meyer et al. 1978). Swine are large animals, where multiple wounds/insertions of cannulas are possible without interfering with each other. However, swine as an animal model is associated with higher costs and due to the large size, it is difficult to handle. There are many similarities to humans and that is why it is used as an appropriate model for human skin and adipose tissue wound healing (Sullivan et al. 2001, Seaton et al. 2015). Swine studies are 78 % consistent with human studies of wound healing, whereas other animal models have a lower rate (Seaton et al. 2015). Comparable skin characteristics are a thick epidermis (swine: 30 – 140 µm; human: 50 – 120 µm), and a dermis containing a lot of elastic fibers and immune cells (Sullivan et al. 2001, Seaton et al. 2015). There are similarities in epidermal enzyme pattern and tissue turnover time. Moreover, it has a sparsely-haired coat, similar immune and dendritic cells and the blood vessels in the dermis are similarly oriented and distributed (Meyer et al. 1978, Sullivan et al. 2001, Wang et al. 2001, Seaton et al. 2015). Wounds are closed via reepithelialization in swine as well as human (Sullivan et al. 2001). It is important to mention that the porcine skin does not completely correspond with the human skin. There are some differences such as the fact that hair follicles in the human skin are more vascularized. Contrary to humans, swine skin contains apocrine sweat glands while humans have eccrine sweat glands everywhere on the body (Seaton et al. 2015).

1.6 Real-time quantitative polymerase chain reaction (qPCR)

qPCR is a feasible tool for the analysis of gene expression and is widely used in routine diagnostics and scientific disciplines like molecular biology, pharmacology and medicine (Jozefczuk and Adjaye 2011). It works just like a regular PCR but, additionally, the obtained DNA can be quantified in real-time. This method allows the amplification process to be monitored continuously via fluorescent reporter dyes. The fluorescent signal increases proportional with the amount of the PCR-products (see Figure 3 and Figure 4) (Holzapfel and Wickert 2007, SA Biosciences 2008, Jozefczuk and Adjaye 2011). FRET probe, TaqMan probe, LUX Primer, Molecular Beacon and SYBR Green are examples for possible detection techniques (Holzapfel and Wickert 2007, SA Biosciences 2008).

In this thesis, SYBR Green was used in qPCR to detect PCR products. The fluorescent dye “SYBR Green” binds to the minor groove of double-stranded DNA (Holzapfel and Wickert 2007). SYBR Green has a high sensitivity but a low specificity and binds under adverse conditions not only to the target sequence but also to primer dimers and PCR-byproducts. An increase in the fluorescent signal due these non-specific bindings must to be avoided. Therefore, high-quality primers are essential (Holzapfel and Wickert 2007, SA Biosciences 2008). An analysis of the melting curve after the performed qPCR can be used to verify the specificity of the PCR-products (Holzapfel and Wickert 2007, Jozefczuk and Adjaye 2011). In contrast to SYBR Green, detection techniques with probes are vice versa - expensive, high specificity, low sensitivity (Holzapfel and Wickert 2007, SA Biosciences 2008).

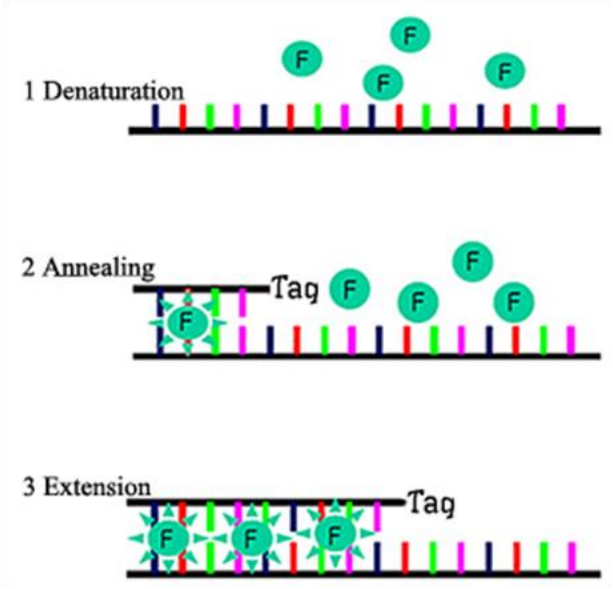

Figure 3: SYBR Green qPCR: Basic principle of qPCR with the processing steps: denaturation, annealing and extension with the fluorescent dye “SYBR Green”. The figure was taken from Sino Biological Inc., 2016.

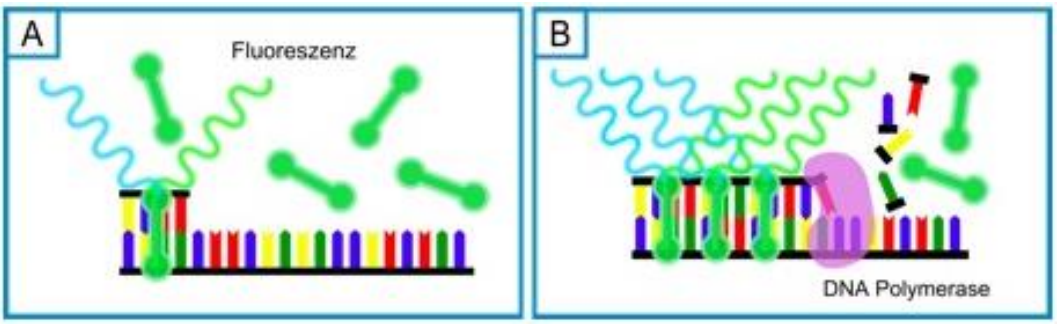

Figure 4: Intercalation of SYBR Green dye:
A: Non-specifically binding of SYBR Green to double-stranded DNA,
B: Amplification of DNA leads to an increase in PCR products and hence, more SYBR Green can bind to DNA, which increases the emission of the fluorescence light.
The figure was taken from International Union of Food Science and Technology (IUFoST), 2013.

qPCR is a method to quantify the amount of mRNA transcripts. To compare the transcription levels, a normalization with stable reference genes (internal standards) is important and a routinely way. For this, the reference genes need to be accurately quantified to normalize the differences in the amount of the amplified samples (Nygard et al. 2007). In Nygard et al., nine reference genes in 17 porcine tissues were investigated. It was determined that β-actin and ribosomal protein L4 (RPL4) have the best expression stability across tissues, whereas β-2-microglobulin and glyceraldehyde-3-phosphate are the least stable ones.

1.7 Genes used for identification of hypoxia and neovascularization

Not much is known about how the immune system responds to the insertion of catheters and how it affects hypoxia, angiogenesis and/or vascularization near the point of trauma. In order to design optimal O_2-based glucose sensors the knowledge of how oxygen supply changes in the vicinity of a catheter is of interest. In this thesis seven markers for hypoxia and/or neovascularization were investigated.

1.7.1 Transforming growth factor beta (TGF-β)

Homodimeric TGF-β is a cytokine, which contains two polypeptide chains (each 12.5 kD) linked by a disulfide bond (Postlethwaite et al. 1987). A major role of TGF-β is to regulate tissue repair and regeneration of tissue after injury. It is present as an inactive precursor which becomes mature and active by being proteolytically cleaved. In total, there are three isoforms, TGF-β1, 2 and 3, which are similar to each other in structure and function. High concentrations are present in platelets (Border and Ruoslahti 1992). TGF-β is involved in many events in the healing process, from tissue injury to wound healing; Angiogenesis is induced, fibroblasts are stimulated (Roberts et al. 1986) and monocytes

are chemoattracted (Wiseman et al. 1988) for example. Other effects of TGF-β are the synthesis of fibronectin (Postlethwaite et al. 1987) and the induction of scarring and fibrosis (Border and Ruoslahti 1992). Several inducers for angiogenesis exist, which are divided into three groups. TGF-β belongs to the third group, the indirect-acting factors, which are responsible for the release of direct-acting factors from different kinds of cells to induce angiogenesis (Liekens et al. 2001).

1.7.2 Vascular endothelial growth factor (VEGF)

The growth factor VEGF has a molecular weight of 45 kDA and is a disulfide-linked homodimeric glycoprotein (Carmeliet 2005). VEGF, also known as vascular permeability factor (Dixelius et al. 2006), is one of six members of the VEGF family and it is involved in the regulation of vasculogenesis and wound healing (Liekens et al. 2001, Hausman and Richardson 2004). Additionally, VEGF is involved in other events like induction of endothelial cell proliferation or permeabilization of blood vessels, inhibition of apoptosis and promoting cell migration (Murphy and Fitzgerald 2001). Many cell types and different tissues express VEGF. Moreover, expression of VEGF is induced by hypoxia whereas VEGF expression is reduced by normoxia (Liekens et al. 2001). $VEGF_{165}$ is the most abundantly isoform generated through alternative exon splicing (Liekens et al. 2001, Murphy and Fitzgerald 2001). VEGF belongs to the first group of angiogenesis inducers. In the first group are inducers that affect endothelial cells (Liekens et al. 2001).

1.7.3 Hypoxia-inducible factor-1 alpha (HIF-1α)

HIF-1α is one of three subunits of HIF-1, a heterodimeric transcriptional activator dependent on oxygen and involved in angiogenesis. The other subunits are HIF-2α and HIF-3α (Lee et al. 2004, Higgins et al. 2007). Hydroxylation, acetylation and phosphorylation are post-translational modifications which are necessary for the regulation of HIF-1α stability and activity. Under normoxic conditions the HIF-1α subunit is degraded quickly, whereas under hypoxic conditions it is stable. HIF-1, the major regulator of oxygen, is important in systemic oxygen homeostasis (Lee et al. 2004). It stimulates the expression of gene products (such as VEGF) required to induce angiogenesis and erythropoiesis to enhance the availability level of oxygen in the cellular environment (Lee et al. 2004, Higgins et al. 2007).

1.7.4 Platelet-endothelial cell adhesion molecule-1 (PECAM-1 or CD31)

PECAM-1 or CD31 in its mature form, has 130 kDA molecular weight. It is expressed on (vascular) endothelial cells, platelets and leukocytes, primarily on monocytes and neutrophils (Newman 1994, Newman and Newman 2003, Feng et al. 2016). Only a small amount of PECAM-1 is present on platelets, whereas nearly 200 times more are expressed on the surface of endothelial cells (Newman 1994). As PECAM-1 is highly constitutively expressed in a state of rest or non-adhesion, an event of activation (e.g. phosphorylation) is necessary for the molecule to become functional. It plays an important role in the process of inflammation in which it recruits leukocytes to inflammatory sites (Delisser et al. 1994). It is involved in blood vessel formation, and thus in the process of angiogenesis. In molecular biology, CD31 is used as a marker of angiogenic blood vessels (Delisser et al. 1994, Newman and Newman 2003). Additionally, it participates in vessel repair, in which it is responsible for the migration of endothelial cells (Feng et al. 2016).

1.7.5 Matrix metalloproteinase 2 (MMP2)

MMP2 is a zinc-containing endopeptidase with a molecular weight of 72 kDA that is secreted as a proenzyme. It is also called gelatinase A or type IV collagenase and belongs to the matrix metalloproteinase family, in which approximately 20 members have been identified. All of them possess a Zn^{2+}-dependent catalytic site (Ben-Yosef et al. 2002, Sariahmetoglu et al. 2017).

MMP2 is involved in the process of extracellular matrix remodeling during angiogenesis and wound healing. There are two possible ways to activate fully mature MMPs, either via proteolytic cleavage or post-translationally (Sariahmetoglu et al. 2017). MMP2 is present on most tissues and cells, like endothelial cells and cells which form vascular walls (Ben-Yosef et al. 2002, Sariahmetoglu et al. 2017). Regulation of MMP2 enzymatic activity is dependent on the status of its phosphorylation. There are two hypotheses regarding its activity: either only a small fraction of possible phosphorylation sites are necessary to achieve enzymatic activity, or multiple sites need to be phosphorylated having opposing effects (Sariahmetoglu et al. 2017).

Ben-Yosef et al. found that hypoxia-related endothelial cell migration and death is dependent on MMP2. Consequently, MMP2 not only has a proangiogenic, but also an apoptotic role in a hypoxic microenvironment (Ben-Yosef et al. 2005).

1.7.6 Integrin alpha M (ITGAM or CD11b)

Integrin alpha M or CD11b is one of three possible α-subunits of CD11/CD18 adhesion receptors, which are surface-membrane glycoproteins promoting leukocytes to interact with other leukocytes or endothelial cells. CD11a, b or c are the three possible α-subunits that are non-covalently linked to CD18, the β-subunit, forming the heterodimeric receptor. This receptor is expressed on polymorphonuclear cells and monocytes. In these cells proinflammatory functions are mediated by CD11/CD18 (Dana et al. 1991). In the skin CD11b is expressed by Langerhans cells and dermal macrophages (Minutti et al. 2017), but the heterodimeric glycoprotein is also expressed on monocytes/macrophages, neutrophils, dendritic cells or natural killer cells. CD11b/CD18 plays a role in cell activation, phagocytosis, chemotaxis, cytotoxicity and it has a crucial role in inflammation (Solovjov et al. 2005, Fossati-Jimack et al. 2013). Additionally, CD11b is expressed on myeloid cells. Tumor-infiltrating $CD11b^{+}$ myeloid cells express proangiogenic factors, such as VEGF, and thus, promote angiogenesis (Avraamides et al. 2008, Ahn et al. 2010). When a tumor is depleted by irradiation, which inhibits angiogenesis, vasculogenesis and CD11b cells are important for the tumor recurrence (restoration of tumor vascular and tumor regrowth) (Ahn et al. 2010).

1.7.7 Fibronectin (FN)

The glycoprotein fibronectin is an adhesive molecule that is involved in various stages of the wound healing process and it is important in cell-matrix interactions. Cellular adhesion is its key role, but fibronectin is also responsible in cell migration and the mediation of cell growth. This glycoprotein is present on many tissues and the functional domains are the same throughout all fibronectin molecules. The gene encoding fibronectin consists of three types or modules – type I, type II and type III. Type I binds to fibrin, type III binds to cells and Type II is present in domains of collagen-binding. Due to the ability of function and binding, given by these modules, fibrin is able to interact with cytokines and other cell types. Plasma and cellular or tissue fibronectin are the two existing forms. Plasma fibronectin produced by hepatocytes acts in the early phase of wound healing. The formed fibrin clot is strengthened via the binding of fibronectin to fibrin and platelets (Lenselink 2013). In the later phase of wound healing the fibrin clot is invaded by fibroblasts and endothelial cells, initiating lysis of the clot. Cellular fibronectin is deposited by these cells and granulation tissue is formed and vascularized (Tonnesen et al. 2000, Lenselink 2013).

2. Aim

The aim of this master thesis was to determine whether certain genes that relate to tissue hypoxia and/or neovascularization are expressed similarly around the center and the tip of a continuous subcutaneous insulin infusion (CSII) catheter. Furthermore, it was investigated whether neovascularization and oxygenation changes in the course of seven days of catheter wear-time. Thirdly, this thesis compared vascularization and hypoxia around the two most commonly used materials for insulin infusion systems: steel and Teflon.

3. Materials and Methods

3.1 Materials

3.1.1 Insulin Infusion Sets (CSII catheters) and Insulin Pump

Product	Company
Quick-set (Teflon) 6 mm	Medtronic plc, Ireland
Sure-T (Steel) 6 mm	Medtronic plc, Ireland
Pump (Medtronic Paradigm)	Medtronic plc, Ireland

3.1.2 For Animal Studies:

Product	Company
Regular soap, alcohol wipes and medical gauze	
Kinesiology tape (Leukotape K 5 cm x 5 m)	BSN medical, Vienna, Austria
Stockinette (tg soft 10 m Size M)	Lohmann & Rauscher International GmbH Co. KG, Vienna, Austria
OPSITE Medical Dressing	Smith & Nephew, London, UK

3.1.3 mRNA Analysis - Sampling

Product	Company
2 ml Eppendorf tubes	
Disposable scalpels and forceps	
RNA*later*®	Sigma-Aldrich®, St. Louis, MO, USA
RNA*se* AWAY™ spray	Thermo Fisher Scientific Inc., Waltham, MA, USA

3.1.4 mRNA Analysis - qPCR

Product	Company
MagNALyser Green Beads	Roche Applied Science, Penzberg, Germany
QIAzol Reagent	Qiagen, Venlo, Netherlands
RNeasy Mini Kit	Qiagen, Venlo, Netherlands
Reverse Transcriptase Kit	Applied Biosystems®, Thermo Fisher Scientific Inc., Waltham, MA, USA
Primers for porcine markers of inflammation, vascularization and oxygenation	Sigma-Aldrich®, St. Louis, MO, USA
Roche LightCycler® Instrument	Roche Applied Science, Penzberg, Germany
LightCycler® 480 SYBR Green I Master	Roche Applied Science, Penzberg, Germany
LightCycler® 480 Multiwell plate 384, clear	Roche Applied Science, Penzberg, Germany

3.1.5 Devices

MagNALyser	Roche Applied Science, Penzberg, Germany
LightCycler® 480 System	Roche Applied Science, Penzberg, Germany

3.1.6 Software

- Primer design: Primer3Plus (http://www.bioinformatics.nl/cgi-bin/primer3plus/primer3plus.cgi)
- qPCR analysis: LightCycler® 480 Software (Roche Applied Science, Penzberg, Germany)
- Data evaluation:
  - Microsoft Excel 2013
  - GraphPad Prism 5.0 (GraphPad Software, San Diego, USA)
  - SPSS version 23.0 (SPSS Inc., Chicago, IL)
  - https://www.graphpad.com/quickcalcs/grubbs1/ to remove outliers

3.2 Research Design and Methods

According to Austrian law and ethical regulations, an animal study with ten female farm swine (sus scrofa domesticus) was performed in order to investigate the influence of steel and Teflon cannulas on hypoxia and/or vascularization in the adipose tissue for a period of 7 days of catheter wear-time. This study was approved by the Austrian Federal Ministry of Science, Research and Economy (GZ: BMWFW-66.010/0073-WF/V/3b/2016) and performed in consent with Directive 2010/63/EU on the protection of animals used for scientific purposes.

The swine used for the study were four months old and had an average weight of 45 ± 5 kg. The supplier of the animals was farmer Franz Zehenthofer, Wohldorf 25, 8521 Wettmannsstätten, Austria (LFBIS-Nr: 3201953).

3.2.1 Animal care

Seven to 10 days before the study started, the animals arrived at the animal facility (Institute for Biomedical Research, Medical University of Graz) in order to allow the animals to adjust to the new environment. Animals were housed in pairs until the day of study and were separated after the first catheters were inserted to avoid catheter manipulation by the animals. Well-being and health condition of the animals, as well as catheter sites, were checked regularly.

3.2.2 Insertion of catheters

In total, the experiment was performed over a period of 8 days. Catheters were inserted on day 1 (7 days of wear-time), day 4 (4 days of wear-time) and day 7 (1 day of wear-time) along the spine. This area was chosen to avoid catheter loss due to rubbing and direct pressure on the catheters from laying on them. The animals were sedated, shaved and washed on day 1. Water and soap was used to clean the skin. Afterwards the skin was disinfected and a layer of transparent medical adhesive was placed onto the skin in order to enable better catheter adhesion as well as to prevent catheter loss caused by movement or friction. Two catheters (1 Medtronic Sure-T®, 6 mm steel and 1 Medtronic Quick-set®, 6mm Teflon), were inserted into the subcutaneous adipose tissue per time point, see Figure 5. After insertion, each hub of the Quick-sets was directly connected to an insulin pump, which contained a reservoir filled with saline.

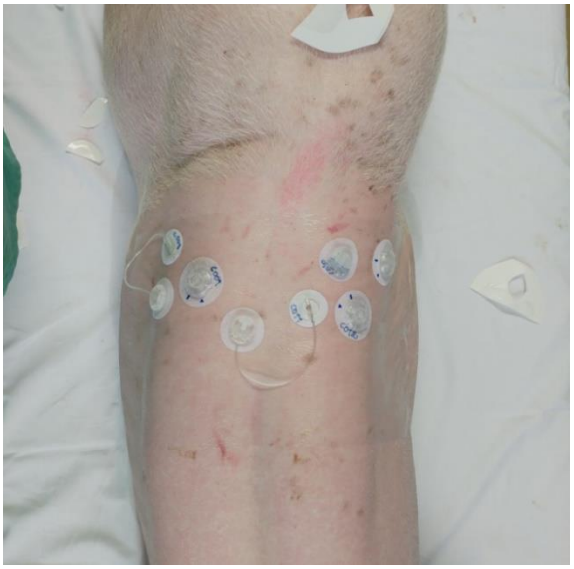

Figure 5: Insertion of catheter: Two catheters, one Teflon and one steel, were inserted into the subcutaneous adipose tissue per time point.

To be sure that no catheter kinked during insertion, a bolus of 3 - 4 units [30 - 40 µl] of saline was infused. After the bolus had been set, the insulin pump was disconnected. The catheter hub was sealed with a plastic cap to prevent contamination. A piece of medical gauze, followed by another layer of medical adhesive and a Kinesiology tape was used to fix the inserted catheter for the whole duration of the study. Additionally, a stockinette with four holes was pulled over the animal's body, see Figure 6. To avoid friction on the legs by the stockinette, the edges were padded with cotton.

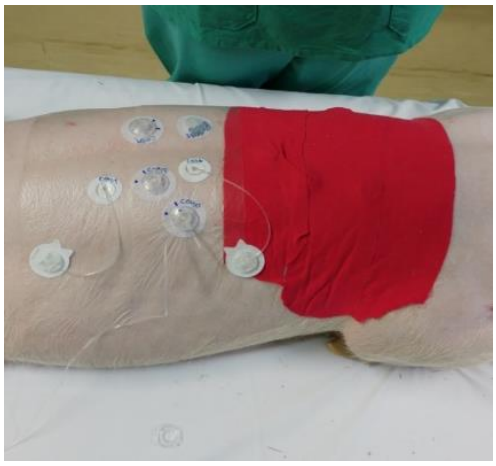

Figure 6: Covering of catheters: After insertion of catheters, they were fixed using (A) a piece of gauze, a layer of medical adhesive and a Kinesiology tape.

Sedation was performed on days 4 (wear-time = 4 days) and 7 (wear-time = 1 day) followed by removal of the stockinette and insertion of further CSII catheters. On the other days (2, 3, 5 and 6), the animals were able to move freely in their pens.

Before the tissue was excised around the catheter sites on day 8, the swine were euthanized.

In total, 60 catheters, 30 steel and 30 Teflon, were inserted and the samples were used for quantitative real-time PCR in this thesis.

Table 1: Study Design.

Study day number	Catheters	Wear-time
1 (Fri)	2	7 days
2 (Sat)		
3 (Sun)		
4 (Mon)	2	4 days
5 (Tue)		
6 (Wed)		
7 (Thu)	2	1 day
8 (Fri)	Tissue excision	

3.2.3 Excision of adipose tissue

On the last day of study (day 8) the adhesives were carefully removed. Tissue was grossed down to about 0.5 cm distance from the catheter. A piece of fatty tissue from around the catheter tip (approx. 5 x 5 x 5 mm) and around the shaft was removed and placed immediately in RNAlater solution. Samples were stored at 4 °C overnight before transferring them to – 80 °C until RNA isolation.

In order to relatively compare gene expression under traumatic conditions to non-traumatic conditions, a piece of reference tissue was excised as well.

3.2.4 RNA isolation from adipose tissue with MagNA Lyser Green Beads (Roche)

The following protocol was used for RNA isolation from adipose tissue:

Cool the centrifuge to 4 °C. All Steps with TRIzol/QIAzol are done under the fume hood.

1. Small pieces (appr. 0.5 x 0.5 x 0.5 cm) of tissue are taken with a tweezer from the RNAlater into tubes prefilled with beads
2. Cover the filled tubes with 1 ml TRIzol (pink) and centrifuge them for 20 sec and 6500 rpm (MagNA Lyser settings)
3. Shake the tubes alternately in MagNA Lyser and incubate them on a block of ice for 1 min (repeat 3 times)
4. Incubate the tubes for 5 min at room temperature

5. Centrifuge the tubes for 10 min at maximum speed
6. Carefully remove the fatty layer
7. Add 200 µl chloroform to each sample and vortex the tube thoroughly
8. Incubate the tubes for 2 - 3 min at room temperature
9. Centrifuge them for 15 min at maximum speed and 4 °C
10. Remove the supernatant and transfer it to a new tube
11. Add 0.5 ml isopropyl alcohol and mix it upside down (20x)
12. Incubate the tube for 10 min (max. 15 min) at room temperature
13. Centrifuge them for 10 min at max. 12,000 x g (4 °C)
14. Remove the supernatant (Do not remove the pellet!)
15. Add 1 ml 75 % EtOH and vortex
16. Centrifuge for 10 min at max. 12.000 x g (4 °C) and preheat the heating block
17. Remove the supernatant (Remove ethanol residues carefully! – dab on pulp)
18. Let the pellet dry on air (~ 20 min) until it is transparent
19. Dissolve the pellet in 20-50 µl RNase free water (depended on the size of pellet and cell type)
20. If the pellet is too big and cannot be dissolved: Heat it up for 5 min at 65 °C on the heating block and mix thoroughly by pipetting
21. Afterwards put RNA immediately on ice!
22. Measure the RNA-concentration via NanoDrop
23. Store RNA at – 80 °C

3.2.5 cDNA synthesis

The following protocol was used for translation of RNA into cDNA:

2x RT master mix for 1 RNA sample (in µl):

10x RT buffer	2.0 µl
25x dNTP mix (100 mM)	0.8 µl
10x RT random primers	2.0 µl
MultiScribe RT [50 U/µl]	1.0 µl
nuclease-free water	4.2 µl
	10.0 µl

Reverse transcription:

1. 10 µl RNA sample (to equal concentration – 500-2000 ng in 10 µl – appropriately diluted in nuclease free water
2. 10 µl of 2x RT master mix
3. Mix thoroughly by pipetting; centrifuge

Thermocycler settings:

	Step 1	Step 2	Step 3	Step 4
Temperature	25 °C	37 °C	85 °C	4 °C
Time	10 min	120 min	5 min	∞

Afterwards dilute samples with 30 µl (at 500 ng of RNA used), 80 µl (at 1,000 ng of RNA used) or 180 µl (at 2,000 ng of RNA used) nuclease free water.

cDNA samples were stored at – 20 °C.

3.2.6 Quantitative Real-time PCR (qPCR) with SYBR Green

qPCR was performed on each sample in triplicates.

1x master mix (per well):

SYBR Green MM 2x	5.0 µl
Forward primer (10 pmol/µl)	0.5 µl
Reverse primer (10 pmol/µl)	0.5 µl
cDNA (20 ng)	2.0 µl
ddH2O	2.0 µl
total	10.0 µl

1. Prepare master mix
2. Prepare plate and foil for Roche 480 LightCycler® system
3. Place 2 µl of cDNA (concentration: 1 ng/µl) in plate per well (triplicates)
4. Pipette 8 µl of master mix to each well (in total 10 µl per approach)
5. Centrifuge plate and place it in Roche 480 LightCycler® system
6. Start the LightCycler program:
   Detection Mode: Mono Color Hydrolysis Samples/UPL Sample
   Reaction volume: 10 µl

qPCR settings:

	Target (°C)	Acquisition Mode	Hold (hh:mm:ss)	RampRate (°C/s)	Cycles	Analysis Mode
Incubation	50	None	00:02:00	4.4	1	None
Denaturation	95	None	00:10:00	4.4	1	None
Amplification	95 60	None Single	00:00:15 00:00:30	4.4 2.2	50	Quantification
Cool	40	None	00:00:10	2.2	1	None

The relative changes in gene expression were calculated from the data obtained by the Roche 480 LightCycler® system using the ΔΔCt method (Equation 1). The cycle threshold (Ct) value of a target gene is compared with Ct values of reference genes. Reference genes are housekeeping genes, which are constantly expressed in the cell. Cellular mRNA data was normalized using internal controls (ribosomal protein 4 (RPL4) and tyrosine 3-monooxygenase/tryptophan 5-monooxygenase activation protein zeta (YWHAZ)).

Equation 1: Calculation of the fold-change in gene expression using the ΔΔCq method

$$\Delta Ct1 = Ct_{C,x} - Ct_{C,hk} \quad (1.1)$$

$$\Delta Ct2 = Ct_{T,x} - Ct_{T,hk} \quad (1.2)$$

$$\Delta\Delta Ct = \Delta Ct1 - \Delta Ct2 \quad (1.3)$$

$$\Delta fold = E^{-\Delta\Delta Ct} \quad (1.4)$$

Ct	…	cycle threshold
T	…	Traumatized tissue (catheter)
C	…	Control tissue (no catheter)
x	…	Gene of interest
hk	…	Housekeeping gene (reference)
Δfold	…	gene expression fold change
E	…	Efficiency of primer pair (ideally 2)

3.2.7 Statistical Analyses

All analyses were based only on available data and conducted using SPSS version 23.0. GraphPad Prism version 5.0 was used for visualization and graph design. Continuous qPCR data (fold change) were tested for normality using visual data inspection and the Shapiro Wilks tests with Lilliefors significance correction. Generalized linear mixed models (GLMM) were applied to investigate the interaction of materials, days of wear-time and location along the catheter (tip versus center). The model selection process to define the appropriate covariance structure was based on an index of relative goodness-of-fit to model the subject variation. P-values were adjusted for multiple testing with Bonferroni correction and were considered significant when they were less than 0.05.

4. Results

Seven genes that relate to tissue hypoxia and/or neovascularization were investigated in a swine model. In total, 60 CSII catheters (30 steel and 30 Teflon) were inserted into the skin of 10 female farm swine. Only one (Teflon) of these 60 CSII catheters kinked above the adhesive and did not push through the animal's skin. Five of these 60 CSII catheters were accidentally pulled out while removing the medical adhesive. However, the insertion channel of these five samples could be located and samples were used for further investigation. Although the insertion channel could be located, it was difficult to distinguish between tip and center. Therefore, these five samples were used as center samples.

In Nygard et al., several possible reference genes were tested for gene expression. We evaluated five of them with the conclusion that only two of them, ribosomal protein 4 (RPL4) and tyrosine 3-monooxygenase/tryptophan 5-monooxygenase activation protein zeta (YWHAZ), were useful housekeeping genes in our experimental procedure due to their stability under all experimental conditions.

The relative changes in gene expression were calculated using the formulas shown in Equation 1. In the graphs comparing steel versus Teflon, the mean values of tip and center were taken for the relative expression levels.

One of the investigated genes was TGF-β, a cytokine that belongs to class 3 of angiogenesis inducers. As it is shown in Figure 7(A), the relative changes in gene expression of TGF-β around steel CSII catheters were approximately 5 times higher on day 1 compared to normal expression (100 % expression), which is represented as intermitted line. On day 4, there was an increase in the relative expression level to approximately 10-fold ($p > 0.05$, not significant). There was a trend ($p = 0.057$) towards increasing relative expression levels around the tip of Teflon CSII catheters between day 1 and day 7, with the highest level on 7 days of wear-time (approximately 7 times higher than healthy tissue). In comparison, the relative changes in gene expression in the center of a Teflon cannula were not significantly different over time (Figure 7(B)). There was no statistically significant difference between the tip and the center over 7 days of wear-time around both materials. As shown in Figure 7(C), the relative changes in gene expression around steel CSII catheters was significantly higher on day 1 compared to Teflon ($p = 0.011$).

VEGF, which is involved in vasculogensis and wound healing, belongs to class 1 of angiogenesis inducers and was tested as well. The relative expression levels around steel and Teflon CSII catheters were under-expressed over time in both tip and center (Figure 8(A) and (B)). After 1 day of wear-time, the relative changes in gene expression around steel were similar to normal expression in the tip and the center, but declined significantly around the tip between 1 and 7 days of wear-time ($p < 0.0001$). A significant difference is also shown between the tip and center of steel cannulas on day 7 ($p = 0.022$). The relative changes in VEGF expression around Teflon CSII catheters significantly decreased around the tip from 1 to 4 days of wear-time ($p = 0.031$). On 7 days of wear-time, the relative expression level of VEGF in the center of Teflon CSII catheter was significantly higher compared to the tip ($p = 0.002$). As shown in Figure 8(C), there is no statistically significant difference between the two materials. In both samples, the relative expression was slightly below normal expression in non-traumatized, healthy tissue.

Furthermore, HIF-1α was investigated in this animal study. It is a key regulator of oxygen, which is able to induce angiogenesis through stimulation of the expression of the relevant gene products. Independent of material, the relative expression levels decreased between day 1 and day 4 ($p = 0.029$) and day 1 and day 7 ($p = 0.003$) around the cannula to levels of normal expression (data of both materials combined, not plotted). The relative expression levels between tip and center around steel catheters showed no statistically significant difference on all days (Figure 9(A)). HIF-1α expression around the tip of Teflon catheters was elevated on day 1 (approximately 1.3-fold) compared with the expression around the center (approximately 0.9-fold, $p = 0.052$, borderline significant. HIF-1α expression around Teflon was normal (100 %) on days 1 (center), 4 (tip and center) and 7 (tip), whereas expression around the center was lowest on day 7 (approximately 0.7-fold, Figure 9(B)). Expression levels around the center were significantly higher around steel than around Teflon on days 4 and 7 ($p = 0.04$ and $p = 0.005$, respectively) and showed a trend towards higher expression around steel on day 1 ($p = 0.079$). Figure 9(C) shows the comparison of HIF-1α relative expression levels at the site of trauma caused by steel and Teflon catheters. Independent of location, HIF-1α around steel and Teflon showed a decrease in expression over wear-time, whereby around Teflon catheters the levels were slightly lower. Expression levels decreased from 1.9-fold to 1.2-fold around steel and 1.1-fold to 0.9-fold around Teflon. In comparison to Teflon catheters, the relative expression level around steel catheters was approximately 1.8-fold higher on day 1. The difference between materials was statistically significant on day 7 ($p = 0.001$).

Another factor capable of inducing angiogenesis and recruiting leukocytes to the site of inflammation is CD31. Overall, expression of CD31 was close to reference values and did not increase or decrease notably during catheter wear-time (Figure 10(A) and (B)). A decrease is significant around the tip of the cannula when combining the values of both steel and Teflon in the statistical calculation (day 1 vs. day 4, $p = 0.042$ and day 1 vs. day 7, $p = 0.038$). A statistically significant difference was between the tip and the center of steel catheters on day 7 ($p = 0.021$). Additionally, differences were observed around Teflon on day 1 between tip and center ($p = 0.021$) and around the center between 1 and 4 ($p = 0.042$) and 1 and 7 days ($p = 0.022$). The expression levels are significantly different between steel and Teflon Figure 10(C) on day 7 of wear-time, with Teflon samples eliciting higher levels of CD31 ($p = 0.03$). Although statistical significance could be shown for differences over time and between materials, CD31 was not overexpressed at any time point and resembled expression levels in healthy tissue.

Extracellular matrix remodeling/degradation is an important step during angiogenesis and wound healing, which is affected by MMP2, another factor investigated in this thesis. As shown in Figure 11, the expression increases over wear-time around both materials. In comparison, there was normal expression of MMP2 around the tip of steel cannulas, whereas the expression was upregulated around the cannula center on days 4 (1-fold versus 1.8-fold, $p = 0.016$) and 7 (1.3-fold versus 2.1-fold, $p = 0.002$) which is shown in Figure 11(A). The relative changes in MMP2 expression around Teflon increased from normal levels to approximately 2.5-fold on day 7 of wear-time in both tip ($p = 0.048$) and center (not significant, Figure 11(B)). As shown in Figure 11(C), relative expression levels increased 1.7-fold (steel) and 2.2- fold (Teflon) after 7 days of wear-time, whereas on the other days, the expression levels were close to normal expression (100 %).

Although not directly involved in angiogenesis or vascularization, CD11b is nevertheless important for the activation and interaction of various immune cells and processes like phagocytosis. As shown in Figure 12(A) and (B), the relative expression of CD11b around steel and Teflon increased 200 % to 400 % over time compared to reference tissue. This increase is statistically significant around the tip and center of Teflon catheters between 1 and 4 days of wear-time ($p = 0.017$ and $p = 0.044$, respectively) and around the center between 1 and 7 days ($p = 0.044$, Figure 12(B)). The expression of CD11b around the cannula tip was significantly lower around steel than Teflon on all days ($p = 0.025$). Figure 12(C) shows a 4.2-fold increase in the relative expression around Teflon over 7 days. In contrast to Teflon, the relative changes in CD11b expression around steel were

almost stable over time (approximately 2.5-fold higher compared to reference tissue).

The adhesive molecule FN, important for cell-matrix interactions and necessary in several stages in wound healing, was also tested. The relative changes in FN expression around steel significantly increased over time showing the highest levels on 7 days of wear-time in both tip (5.8-fold) and center (4.3-fold, Figure 13(A)). This increase was statistically significant around the center of steel cannulas between 1 and 4 days of wear-time ($p = 0.029$). The relative expression levels of FN around Teflon cannulas increased significantly from day 1 to day 4 and from day 1 to day 7 ($p = 0.024$ around the center). Around Teflon cannulas normal expression was observed on day 1, which increased approximately 5.5-fold around the tip and approximately 3-fold around the center on day 4 and day 7. Comparing the expression of FN around the tip between steel and Teflon, around Teflon the relative expression level was twice as high on day 4 (2.5-fold vs. 5.3-fold, Figure 13(B)). Both materials showed higher expression around the tip than center (not significant). In Figure 13(C), the expression levels of FN were compared between steel and Teflon showing increasing expression levels over time, but not statistically significant over time. On 4 and 7 days of wear-time, the relative changes in FN expression around steel cannulas increased 2.6-fold and 5-fold and around Teflon cannulas approximately 4.3-fold compared to normal.

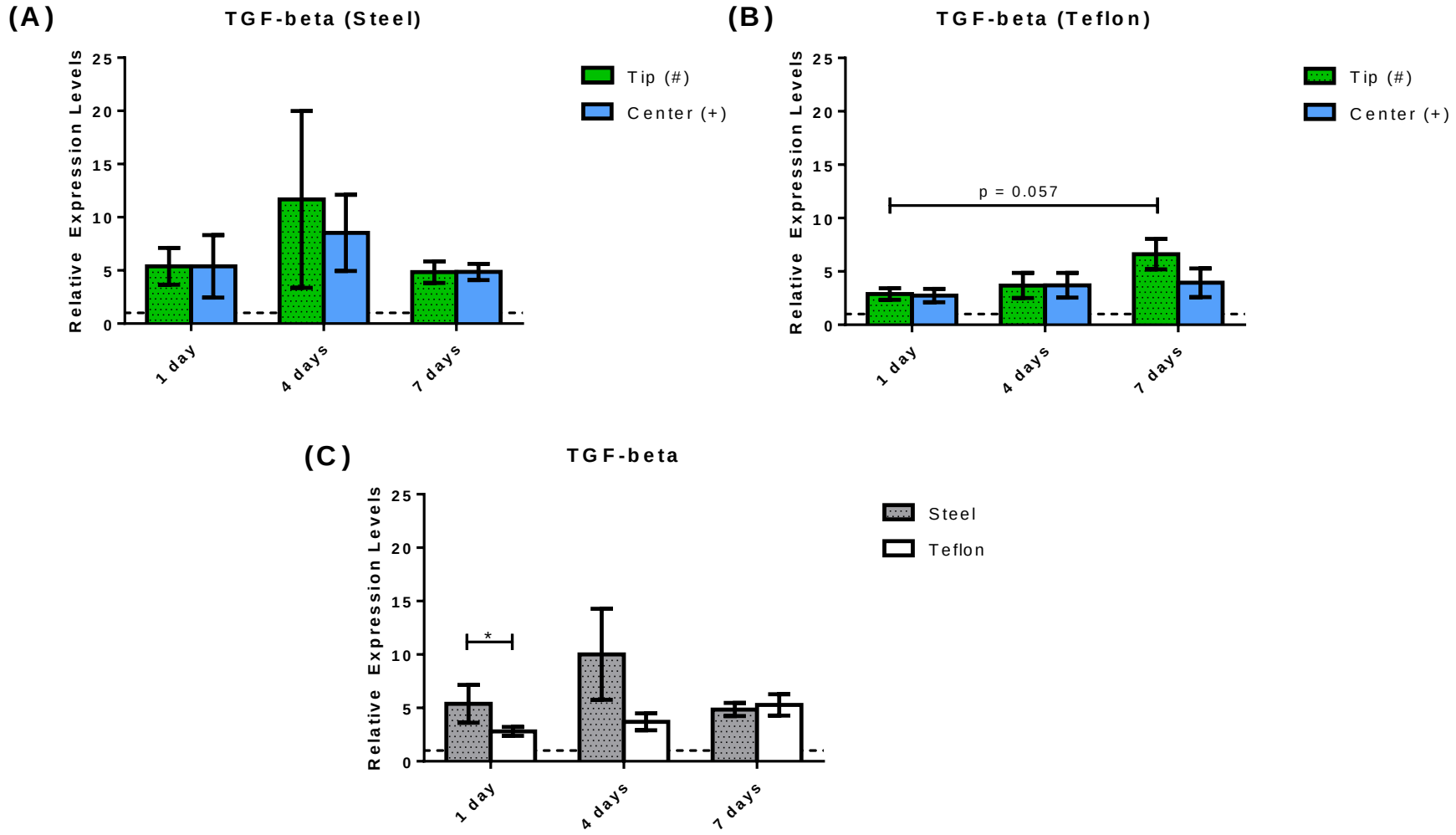

Figure 7: Relative expression levels of TGF-β: Relative gene expression around steel and Teflon CSII catheters on day 1, day 4 and day 7. Comparison between tip and center of (A) steel CSII catheters and (B) Teflon CSII catheters. Comparison of steel versus Teflon CSII catheters is shown in (C). Intermitted line represents normal expression under non-traumatized conditions ($^{\#\#\#/+++}p < 0.0001$; $^{\#\#/++}p < 0.005$; $^{\#/+}p < 0.05$; $^{**}p < 0.005$; $^{*}p < 0.05$; differences between locations or materials). Data are presented as mean ± SEM.

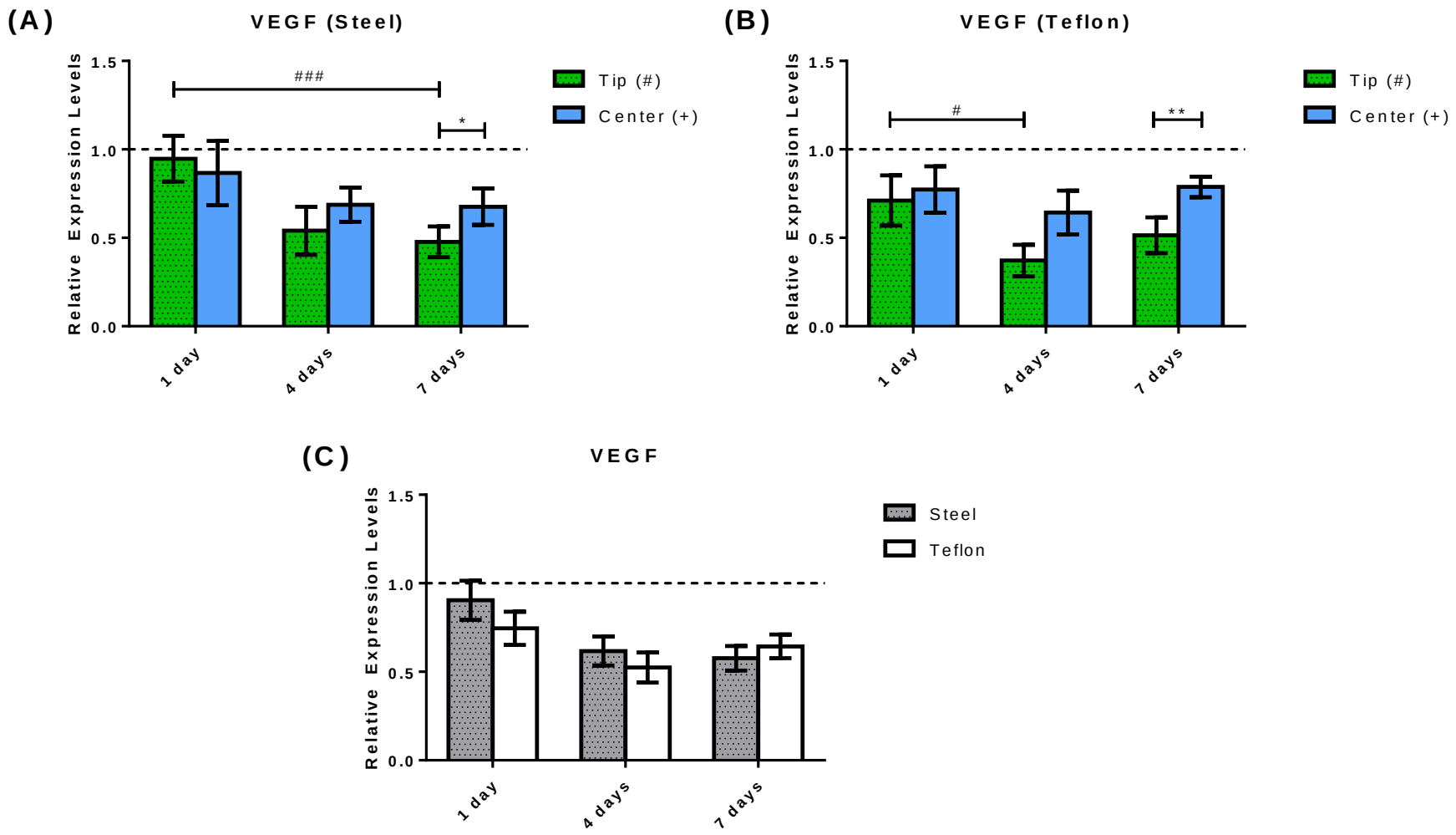

Figure 8: Relative expression levels of VEGF: Relative gene expression around steel and Teflon CSII catheters on day 1, day 4 and day 7. Comparison between tip and center of (A) steel CSII catheters and (B) Teflon CSII catheters. Comparison of steel versus Teflon CSII catheters is shown in (C). Intermitted line represents normal expression under non-traumatized conditions ($^{\#\#\#/+++}p < 0.0001$; $^{\#\#/++}p < 0.005$; $^{\#/+}p < 0.05$; $^{**}p < 0.005$; $^{*}p < 0.05$; differences between locations or materials). Data are presented as mean ± SEM.

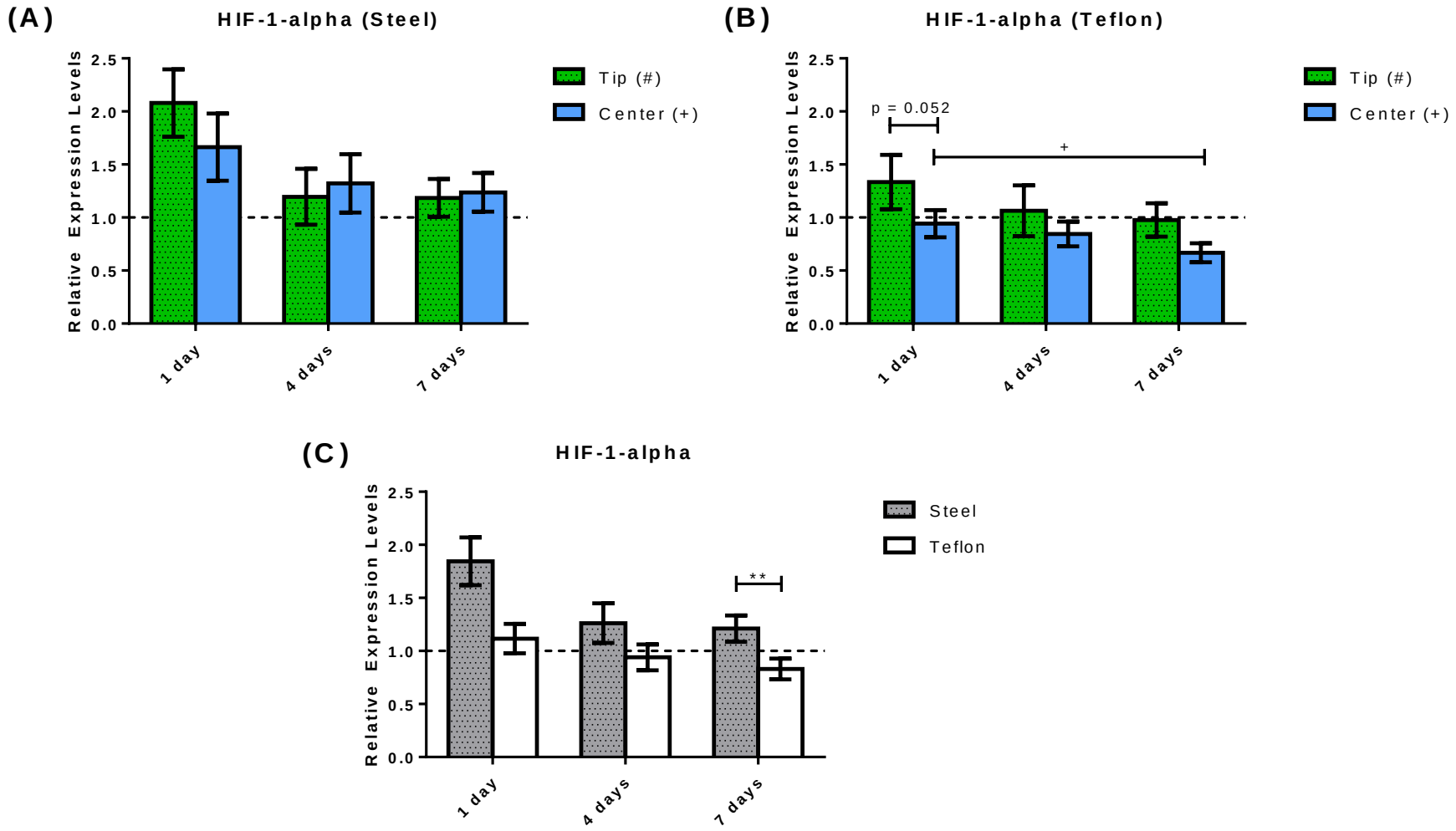

Figure 9: Relative expression levels of HIF-1α: Relative gene expression around steel and Teflon CSII catheters on day 1, day 4 and day 7. Comparison between tip and center of (A) steel CSII catheters and (B) Teflon CSII catheters. Comparison of steel versus Teflon CSII catheters is shown in (C). Intermitted line represents normal expression under non-traumatized conditions ($^{\#\#\#/+++}p < 0.0001$; $^{\#\#/++}p < 0.005$; $^{\#/+}p < 0.05$; $^{**}p < 0.005$; $^{*}p < 0.05$; differences between locations or materials). Data are presented as mean ± SEM.

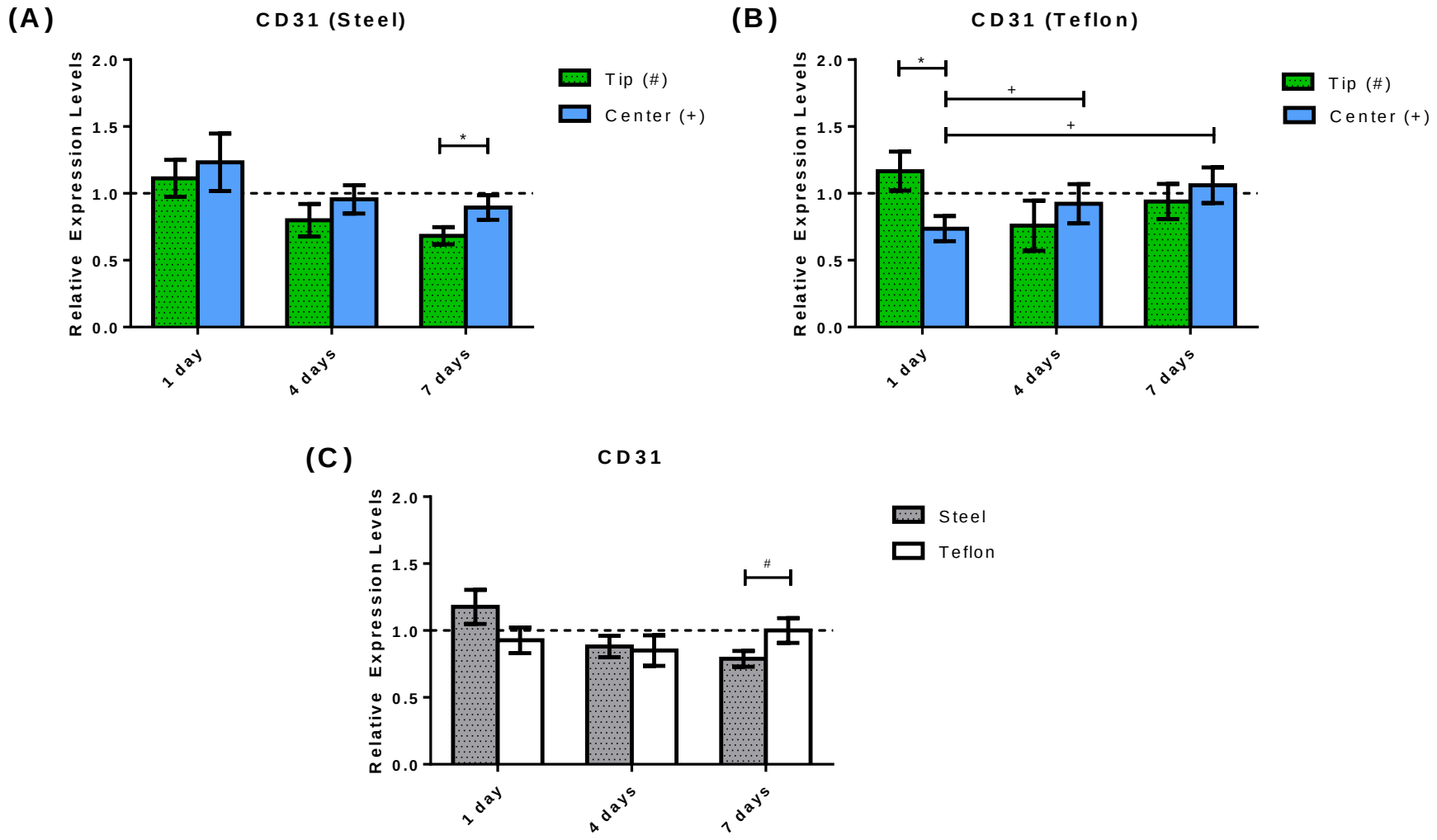

Figure 10: Relative expression levels of CD31: Relative gene expression around steel and Teflon CSII catheters on day 1, day 4 and day 7. Comparison between tip and center of (A) steel CSII catheters and (B) Teflon CSII catheters. Comparison of steel versus Teflon CSII catheters is shown in (C). Intermitted line represents normal expression under non-traumatized conditions ($^{\#\#\#/+++}p < 0.0001$; $^{\#\#/++}p < 0.005$; $^{\#/+}p < 0.05$; $^{**}p < 0.005$; $^{*}p < 0.05$; differences between locations or materials). Data are presented as mean ± SEM.

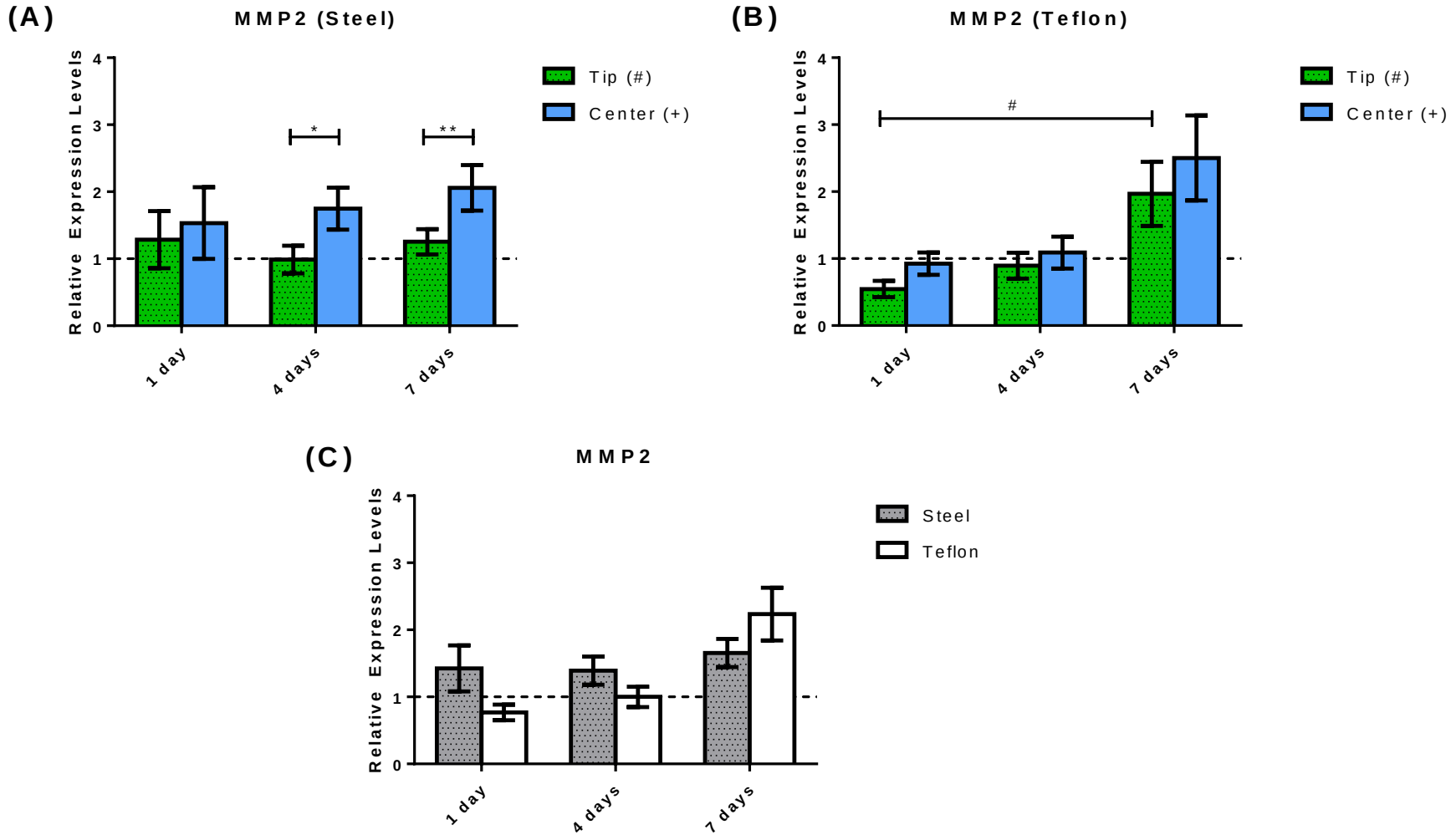

Figure 11: Relative expression levels of MMP2: Relative gene expression around steel and Teflon CSII catheters on day 1, day 4 and day 7. Comparison between tip and center of (A) steel CSII catheters and (B) Teflon CSII catheters. Comparison of steel versus Teflon CSII catheters is shown in (C). Intermitted line represents normal expression under non-traumatized conditions ($^{\#\#\#/+++}p < 0.0001$; $^{\#\#/++}p < 0.005$; $^{\#/+}p < 0.05$; $^{**}p < 0.005$; $^{*}p < 0.05$; differences between locations or materials). Data are presented as mean ± SEM.

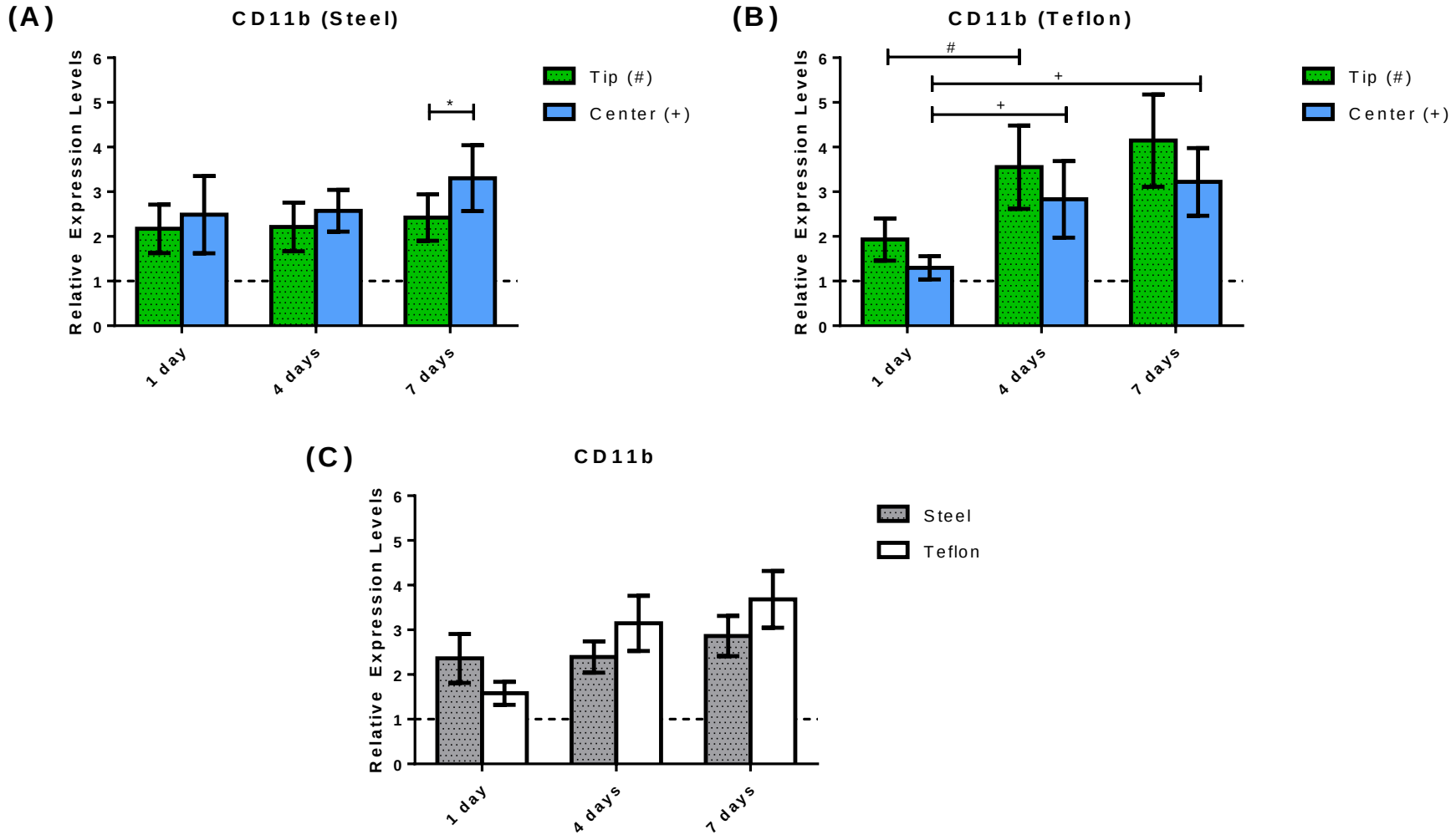

Figure 12: Relative expression levels of CD11b: Relative gene expression around steel and Teflon CSII catheters on day 1, day 4 and day 7. Comparison between tip and center of (A) steel CSII catheters and (B) Teflon CSII catheters. Comparison of steel versus Teflon CSII catheters is shown in (C). Intermitted line represents normal expression under non-traumatized conditions ($^{\#\#\#\#/+++}p < 0.0001$; $^{\#\#/++}p < 0.005$; $^{\#/+}p < 0.05$; $^{**}p < 0.005$; $^{*}p < 0.05$; differences between locations or materials). Data are presented as mean ± SEM.

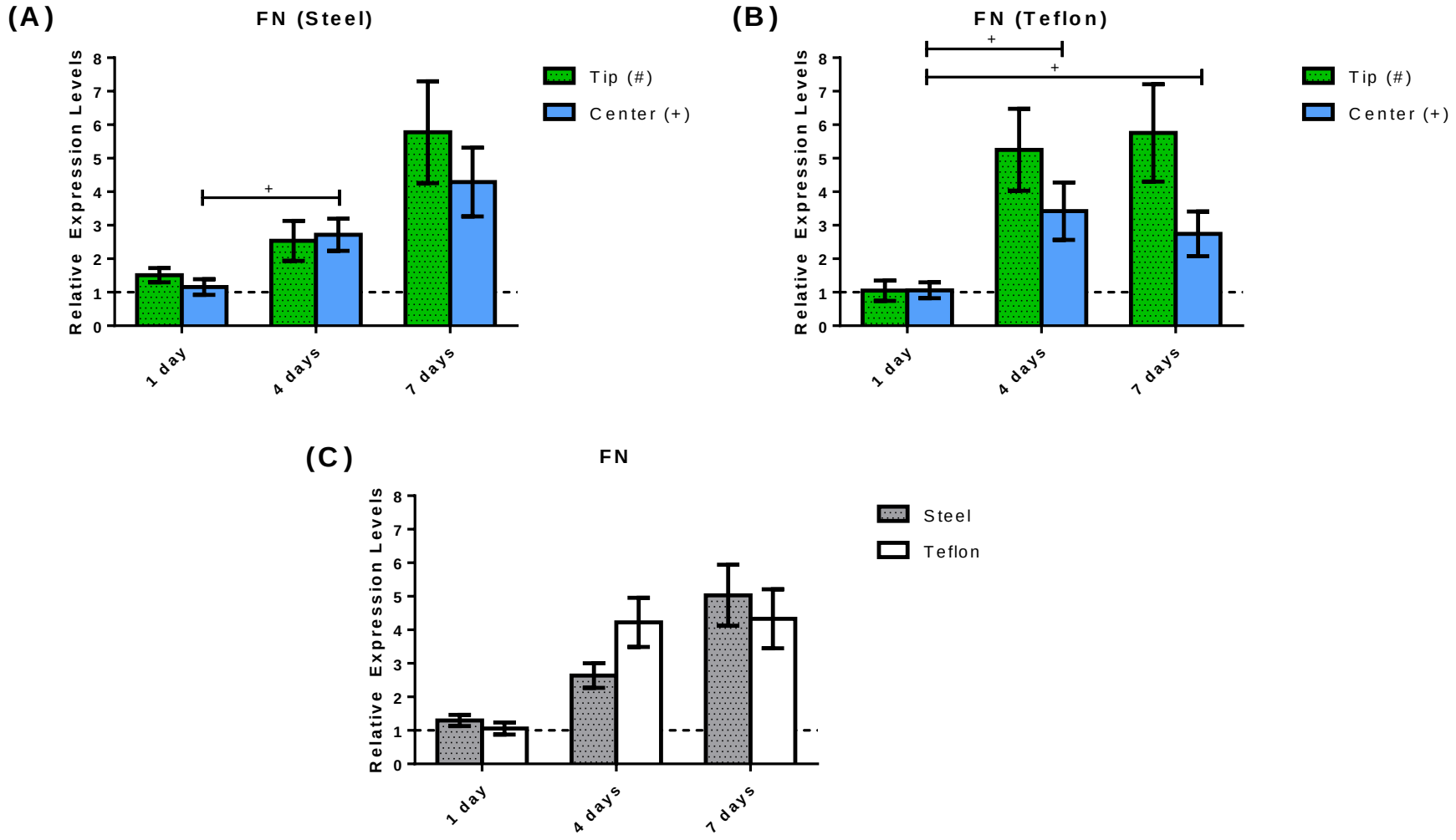

Figure 13: Relative expression levels of FN: Relative gene expression around steel and Teflon CSII catheters on day 1, day 4 and day 7. Comparison between tip and center of (A) steel CSII catheters and (B) Teflon CSII catheters. Comparison of steel versus Teflon CSII catheters is shown in (C). Intermitted line represents normal expression under non-traumatized conditions ($^{\#\#\#\#/+++}p < 0.0001$; $^{\#\#/++}p < 0.005$; $^{\#/+}p < 0.05$; $^{**}p < 0.005$; $^{*}p < 0.05$; differences between locations or materials). Data are presented as mean ± SEM.

5. Discussion

Patients with type 1 diabetes rely on an external supply of insulin and frequent measurement of their blood glucose to ensure normoglycemia (Voet et al. 2002, Chiang et al. 2014, Phillips 2016). There are various available application methods. One such application are continuous subcutaneous insulin infusion (CSII) systems (insulin pump therapy), in which catheters are inserted into the subcutaneous adipose tissue and insulin is continuously supplied via reservoir and plastic tubing. Catheters need to be replaced every 2 to 3 days to ensure an accurate insulin delivery into the tissue (Patel et al. 2014, Heinemann 2016).

Continuous glucose monitoring (CGM) systems have been on the market for more than 15 years. Since then, CGM systems have been constantly extended and improved and measurement inaccuracies minimized (Rodbard 2016). In an artificial pancreas system, CGM and CSII systems communicate with each other based on an algorithm, thus controlling the insulin supply to the tissue (Robert 2013, Thabit and Hovorka 2016). In order to measure the glucose level and to deliver insulin into the body, two devices are necessary at the moment (Ang et al. 2015, Diabetes.co.uk 2017). New research is underway on so-called *single-port systems*, where CGM and insulin infusion are combined in one catheter. In these systems, the glucose sensor is coated onto the insulin infusion catheter (Lindpointner, et al. 2010, Lindpointner et al. 2010 (1), Regittnig et al. 2013, Hajnsek et al. 2014, Ang et al. 2015, Rumpler et al. 2017).

The investigation of the acute immune response to catheter and/or sensor insertion is of interest when it comes to developing improved catheters and CGM sensors. The following questions were attempted to be answered in this thesis:

- How is the oxygen supply distributed in the tissue?
- Is oxygen consumed by immune cells during immune response?
- If oxygen is consumed, does angiogenesis or vascularization occur to balance the oxygen content in the tissue?
- Is the oxygen distribution along the catheter homogenic or heterogenic?

Considering CGM systems such as the single-port system investigated by Rumpler et al., this last question is particularly important. Heterogeneities in vascularization and thus oxygenation along the catheter may substantially influence measurements at the oxygen sensor layers.

When a catheter is inserted into the subcutaneous adipose tissue, it is recognized as foreign and the immune system is activated. As the foreign body is too large to be phagocytized, the immune system will attempt to encapsulate and thereby separate it from the body (Anderson 2001, Ratner and Bryant 2004). It has been hypothesized by Hauzenberger et al. that variable insulin absorption by the adipose tissue is caused by a physical layer around the catheter consisting of immune cells, proteins, collagen and scar tissue and consequently, prevent insulin diffusion into the body (Hauzenberger et al. 2017). In eukaryotic cells, oxygen is consumed for many processes such as tissue- and/or organ-specific functions (Guzy and Schumacker 2006). Shifts in tissue metabolism such as increased consumption of oxygen, depletion of nutrients and generation of ROS and other intermediates also occur in ongoing inflammatory and immune responses (Kominsky et al. 2010). Every cell requires oxygen which is received via diffusion from the blood through the interstitial fluid or when vessels are disrupted through catheter insertion (Pittman 2013).

An animal study with 10 female farm swine was performed to investigate the microenvironment of CSII catheters (steel and Teflon), inserted into the subcutaneous adipose tissue along the spine. The expression levels of seven genes related to hypoxia and/or neovascularization were analyzed.

Areas around steel cannulas showed larger levels of bleeding than those around Teflon cannulas. An explanation for this may be that the steel catheter is rigid and has a sharp tip (Figure 14(A)), whereas Teflon catheters have a blunt end (Figure 14(B)). As a result, small movements are already enough to severely rupture the microvasculature of the adipose tissue (Hauzenberger et al. 2018).

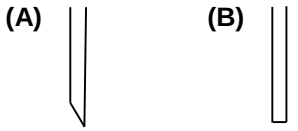

Figure 14: Shape of steel and Teflon cannulas: (A) rigid steel cannula with a sharp tip, (B) flexible Teflon cannula with a blunt end.

TGF-β is crucial in the regulation of tissue repair and tissue regeneration. It is involved in wound healing, fibronectin synthesis, induction of scarring and fibrosis and in many more events (Roberts et al. 1986, Postlethwaite et al. 1987, Border and Ruoslahti 1992). TGF-β induces the production of collagen and is thus directly involved in extracellular matrix remodeling (Werner and Grose 2003). TGF-β gene expression is elevated immediately after insertion independent of the material. Within 24 hours, higher relative

expression levels are observed around steel compared to Teflon. This may be due to the sharp tip of the steel cannula which continuously ruptures tissue and vessels (Matlaga et al. 1976, Lebre et al. 2017, Hauzenberger et al. 2018). Due to the large standard deviation the difference is not statistically significant on day 4, although the average expression of TGF-β is higher around steel than Teflon (10-fold versus 4-fold, respectively). The irregular, but continuous traumatization of the tissue by the sharp tip of steel may lead to these standard deviations. A statistical significance could be achieved by increasing the sample size. A consistent trauma can be observed around Teflon catheters compared to steel. However, after 7 days of wear-time the relative expression levels are approximately equally elevated by 5-fold around both materials, which means that the immune system is equally highly active around both steel and Teflon. Teflon does not seem to injure the tissue as severely as steel after catheter insertion. However, there is a trend ($p = 0.057$) towards increasing relative expression levels around the tip of Teflon cannulas over 7 days indicating consistent tissue regeneration. In Roberts et al., after TGF-β was subcutaneously injected in mice, angiogenesis was induced and fibroblasts were stimulated for collagen production within 2 to 3 days (Roberts et al. 1986). It might also be interesting to analyze TGF-β expression in swine on 2 and 3 days of wear-time, as we could not determine any significant increase or peak in the relative expression levels neither in steel nor in Teflon over time.

TGF-β is also involved in the stimulation of fibroblasts and other cell types which synthesize and secrete components of the extracellular matrix such as FN (Ignotz et al. 1987, Postlethwaite et al. 1987, Parekh et al. 1994). Our results show that the relative expression levels of FN increased over time and as expected, this increase was delayed from TGF-β production. There were no relative changes in FN expression within a day of wear-time but (stimulated by TGF-β) increased greatly after 4 and 7 days of wear-time around both tip and center of steel and Teflon. FN is present during all phases of wound healing. In the beginning, when capillaries are ruptured, bleeding occurs. Bleeding is stopped by the formation of a blood clot containing a network of fibrin and FN as well as other components (Anderson 2001, 2004, Ratner and Bryant 2004, Lenselink 2013). After the provisional matrix is formed, FN is a major factor for cell migration. It is also indirectly involved in wound contraction as it provides a scaffold where components such as collagen fibrils adhere and contract to build a scar. FN is then degraded and collagen deposited, which is necessary for the strength of the scar (Lenselink 2013).

Another purpose of TGF-β is the stimulation of TNF-α and VEGF expression by inflammatory cells (Liekens et al. 2001). However, relating to our data, it could be determined that over 7 days of wear-time VEGF was under-expressed and the relative expression levels of TNF-α (Hauzenberger et al. 2018) were similar or slightly increased compared to expression in non-traumatized tissue. Here, it might be that the expression of these factors is delayed and cannot be observed within 7 days. Additionally, the immune system is a very complex tool of the body and there are many more factors involved than just one in a cascade of reactions or responses. Therefore, one possibility might be, that there are other factors with more influence on VEGF, which are able to downregulate its expression.

VEGF and TNF-α are proangiogenic factors, which are upregulated under hypoxic conditions (Ben-Yosef et al. 2005). As an upregulation of these factors is not observed, it can be assumed that the tissue around the catheters remained normoxic leading to no upregulation within 7 days of wear-time. This is in contradiction with the data obtained from the relative expression levels of HIF-1α around steel (tip and center) and around Teflon (tip) within a day, as HIF-1α is over-expressed, indicating hypoxia in the vicinity of the catheters. The results from 4 and 7 days of wear-time (close to 100 %), however, confirm that normoxic conditions prevailed. As reported by He et al., HIF-1α directly targets the VEGF gene (He et al. 2011).

After the catheter enters the subcutaneous adipose tissue, the immune system immediately sends immune cells and cytokines to the site of injury to combat the foreign body (Anderson 2001, Morais et al. 2010). Relating to our findings on HIF-1α, a large amount of oxygen might be consumed in this initial immune response (defensive reaction), leading to hypoxic conditions and the activation of HIF-1α within a day. Although this difference is not statistically significant, it seems that the steel catheter injures the tissue more severely than Teflon and more oxygen-consuming immune cells are recruited to the site of trauma. HIF-1α has the capability to stimulate many proteins (including VEGF), which are necessary for the induction of erythropoiesis, angiogenesis or vascularization, thereby generating vessels to enhance oxygen availability in the tissue (Lee et al. 2004, He et al. 2011). This could explain the downregulation of HIF-1α expression after time, as HIF-1α is regulated by the oxygen status in the tissue. However, we could not observe an upregulation of VEGF or CD31, both indicators for (new) blood vessels.

FN is important in the process of wound healing, as it is involved in the formation of the extracellular matrix and reepithelialization. It is able to interact with various cell types and cytokines and it also takes part in cell migration and cell growth mediation (Lenselink 2013). FN possesses VEGF binding domains and acts as VEGF cofactor. The biological activity of VEGF is amplified when it binds to FN (Wijelath et al. 2002). These interactions between FN and VEGF is enhanced at acidic pH (Goerges and Nugent 2004). Our data obtained, however, show an opposite effect. FN increases over 7 days of wear-time in both tip and center around steel and Teflon. Based on literature, the relative expression levels of VEGF should also increase, but it remains under-expressed over time. Within 7 days of wear-time, it is not possible to make accurate conclusions about the relation between VEGF and TGF-β, HIF-1α or FN. There are many possibilities why VEGF is under-expressed on 1, 4 and 7 days of wear-time. A possibility could be that VEGF is expressed in a delayed manner, the other possibility could be that the up- and downregulation of VEGF occurred at 2, 3, 5 or 6 days of wear-time. Therefore, a repetition of the whole animal study for a longer duration and with shorter examination intervals might be insightful.

MMP2, like FN, is involved in the remodeling of the extracellular matrix and endothelial cell migration during angiogenesis and wound healing. Expression and activity of MMP2 are enhanced under hypoxic conditions and even more in combination with TNF-α (Ben-Yosef et al. 2005). If we compare the relative changes in gene expression between HIF-1α and MMP2, which are both affected by hypoxia, it is visible that the highest expression level of MMP2 was seen on 7 days of wear-time compared to HIF-1α, where the highest level was already detected within 1 day. A reason for these results could be, that HIF-1α will be activated first under hypoxic conditions while other factors, like MMP2, are activated later on in the immune response. MMP2 expression is even more prominent when both hypoxia and TNF-α are present, which could explain the increasing expression levels over time. In MMP2, the relative expression levels are increasing over time around Teflon approximately 3 - 4 times compared to normal expression while around steel it only increased slightly (approximately 1.5 – 2-fold).

Endothelial cells express CD31, a factor involved in inflammation. It recruits leukocytes onto the site of inflammation and is also involved in the formation of blood vessels (angiogenesis) (Delisser et al. 1994). Neels et al. reported in a fat pad developmental study in mice that CD31-positive neovascularization occurred by day 10, and new microvessels formed already as early as 5 days. qPCR analysis showed that on the 3rd day the expression of CD31 had already increased significantly and reached a plateau

by the 6th day. The increasing amount of mRNA reflects the increasing number of endothelial cells involved in the process of neovascularization (Neels et al. 2004). While a fat pad development is not entirely comparable with the wound healing process discussed in this thesis, it could show at what intervals microvessels are formed and neovascularization occurs. Our results show relative expression levels similar to normal expression or slightly below normal expression around steel and Teflon within 7 days. In steel, it slightly decreased whereas in Teflon it stays nearly constant. If we look at the graphs separately, it is visible that the relative changes in CD31 expression around steel decreased in both tip and center over time. In contrast to steel, the relative expression levels increased over time around the center of Teflon, whereas variable expression (but still close to normal expression) could be detected at the tip. Additionally, CD31 is significantly higher expressed on the tip compared to the center within a day. Perhaps this could be explained by the flexibility of the material, causing the tip to move around more in the tissue compared to more rigid steel. Overall, the CD31 gene expression profile shows that it takes more than 7 days to form neovasculature.

CD11b is one of three possible α-subunits of the adhesion receptor CD11/CD18, which is expressed, for example, on monocytes. It plays a role in the interaction between leukocytes, leukocytes and endothelial cells or leukocytes and certain opsonins bound to invading bacteria and damaged or hypoxic tissues (Dana et al. 1991). CD11b is over-expressed around steel (approximately 2.5-fold) as well as Teflon (1.5 – 3.5-fold). In steel, CD11b is over-expressed and remains relatively constant (tip and center) over wear-time. In an inflicted wound, such as the one caused by inserting a catheter, the recruitment of immune cells (leukocytes, monocytes and so on) takes place to combat the foreign body or pathogens and to close the wound. In this process, CD11/CD18 mediates proinflammatory functions to monocytes and other immune cells, which is also obvious from our data obtained. As $CD11b^{+}$ myeloid cells express VEGF to promote angiogenesis, which we did not observe. Again, we hypothesize that angiogenesis takes place later in (wear-)time.

Angiogenesis and vascularization are important processes in the body to provide sufficiently high amounts of nutrients to cells when there is a need for them. Hypoxia, for example, signals the body to activate angiogenesis by increasing VEGF expression among others (Goerges and Nugent 2004). It would be interesting to learn about the relative changes in CD31 expression (especially by which day neovasculature is present) by extending the study beyond 7 days of wear-time.

After 2 to 3 days of wear-time, it is recommended to replace the catheter of the insulin infusion set. The time points of 1, 4 and 7 days of wear-time were chosen to learn what happens in the tissue immediately after insertion as well as beyond recommended wear-time. We furthermore aimed to increase the probability of detecting differences between the two materials, steel and Teflon, for which we have chosen 4 days of wear-time, as patients usually wear Teflon sets longer than steel sets (Patel et al. 2014). The time point of 7 days of wear-time is of particular interest for the development of closed-loop artificial pancreas systems, where the devices for continuous glucose monitoring have a durability of 7 days (Thabit and Hovorka 2016). As continuous glucose monitoring devices have a longevity of 7 days, the catheters of CSII sets also require a prolonged longevity, when combined in one device. The knowledge of tissue response to CSII catheters after 7 days of wear-time is crucial in the development of single-port devices.

Limitations

A large amount of material was necessary to correctly localize the areas of interest and to obtain sufficiently high amounts of RNA, which was translated to cDNA and used for qPCR analysis. Therefore, we have chosen an animal model with similar characterization and properties of skin and adipose tissue structure like in humans (Sullivan et al. 2001). The swine was the best choice to be used as animal model for our study, however, reactions and responses may differ in humans. In the future, it is necessary to perform a human study as well, as animal tissue does not entirely resemble the human tissue.

It is noteworthy to mention that a limitation of this study was to define “tip” and “center” from the tissue samples along the cannulas. Cutting the tissue in two parts is very subjective, however, this task was always carried out by the same person to minimize errors.

Ten farm swine were used in this study, which is only a small sample size. The sample size could be increased in order to receive more reliable data and decrease standard deviation.

It also has to be taken into account that only a certain amount of proteins can be produced from a single RNA-template, as RNA has a defined half-life (Alberts et al. 2002). Therefore, the amount of RNA differs from the amount of protein present and direct measurements of proteins should be considered as an alternative to analyze factors for tissue oxygenation and vascularization.

6. Conclusion

For the most part, our results show no differences in the relative expression levels between the tip and the center. Additionally, steel compared to Teflon showed no severe differences in the relative expression levels of the examined genes, except for factors usually upregulated under hypoxic conditions (HIF-1α and MMP2). The relative changes in their gene expression vary between the two materials on 1 and 7 days of wear-time, which would have an impact, when O_2-based glucose measurements are carried out, as they are upregulated under hypoxic conditions. Interestingly, factors of angiogenesis (e.g. VEGF) were not activated during the first 7 days of wear-time.

Based on the results obtained and discussed in this thesis, the questions listed above may be answered as follows:

- How is the oxygen supply distributed in the tissue?
    - We found significant differences between tip and center only in some instances and these differences were not consistent over all days of wear-time. We conclude that, for the most part, tissue along catheters is homogenously supplied with oxygen.
- Is oxygen consumed by immune cells during immune response?
    - Factors of hypoxia are upregulated, e.g. HIF-1α shows the highest expression level within a day and decreases afterwards. It can be assumed that in the initial immune response large amounts of oxygen are consumed by immune cells. The decrease over time might be explained as HIF-1α stimulates proteins, which enhances the oxygen availability in the tissue.
- If oxygen is consumed, does angiogenesis or vascularization occur to balance the oxygen content in the tissue?
    - There are no changes in expression of factors involved in angiogenesis or vascularization (VEGF, CD31) observed within 7 days.
- Is the oxygen distribution along the catheter homogenic or heterogenic?
    - Differences between the tip and the center were observed in some instances, but in general, oxygen distribution was homogenic along the catheters. The cannulas have a length of 6 mm, which is short and the distance between the two coated layers is even shorter. Due to the results obtained, the location of the oxygen-sensitive layer and its oxygen-sensitive reference layer coated onto the cannula (a few mm distance) should not have an impact on glucose measurement.

7. Outlook

In new approached single-port systems the glucose level is measured with the help of an O_2-based sensor, where oxygen will be consumed in an enzymatic reaction. Therefore, the change of oxygen level needs to be known in the tissue along the catheters, as heterogenic hypoxic conditions on any day will lead to incorrect measurements.

It may be of interest to repeat the study for a longer period of time, with shorter time intervals for investigation and a larger sample size. As already reported in Roberts et al., induction of angiogenesis and stimulation of fibroblasts occur within 2 to 3 days after exposure to TGF-β. Furthermore, Neels et al. report that neovascularization can be detected by day 10 in mice. It might be interesting to see, by which day neovascularization can be observed in swine or humans. Our time points of 1, 4 and 7 days of wear-time were chosen to get a closer insight into what happens after the CSII catheters need to be replaced. This thesis was an attempt to transfer this knowledge to continuous glucose monitoring devices, which have a longevity of 7 days.

On the current market mostly enzyme-based glucose sensors are available, like in this thesis discussed sensors using glucose oxidase to measure the glucose level. However, there are enzyme-free glucose sensor newcomers based on boronic acid and its derivatives, which are promising alternatives to enzyme-based glucose sensors (Wang and Lee 2015). By choosing sensors that measure glucose independent of oxygen, the acute immune response may have less of an impact on sensor accuracy.

The long-term goal in diabetes technology will be the combination of glucose monitoring and insulin infusion in one device with an extended lifetime to decrease the burden of tedious blood glucose management in patients with type 1 diabetes. The data obtained in this study may be useful for the development of optimized future catheters/sensors/single-port systems. The longevity of CSII catheters or CGM sensors could be extended via coating, masking or modifying the surface of the biomaterial based on the understanding gained about wound healing and inflammation in order to accurately control the responses of bio-reaction. Through this modification, the foreign body reaction could be minimized and normal wound healing could be promoted.

8. Abbreviations

CGM	continuous glucose monitoring
CSII	continuous subcutaneous insulin infusion
FBG cells	foreign body giant cells
FBR	foreign body response
FN	fibronectin
GLMM	generalized linear mixed models
GOx	glucose oxidase
HIF1-α	hypoxia-inducible factor 1-α
ITGAM/CD11b	integrin alpha M
MMP	matrix metalloproteinase
PECAM-1/CD31	platelet-endothelial cell adhesion molecule-1
qPCR	real-time quantitative polymerase chain reaction
ROS	reactive oxygen species
RPL4	ribosomal protein L4
RT	reverse transcriptase
SEM	standard error of the mean
TGF-β	transforming growth factor-β
VEGF	vascular endothelial growth factor

9. Reference List

Ahn, G.-O., Tseng, D., Liao, C.-H., Dorie, M. J., Czechowicz, A., and Brown, J. M., 2010. Inhibition of Mac-1 (CD11b/CD18) enhances tumor response to radiation by reducing myeloid cell recruitment. *Proceedings of the National Academy of Sciences* [online], 107 (18), 8363–8368. Available from: http://www.pnas.org/cgi/doi/10.1073/pnas.0911378107.

Alberts, B., Bray, D., and Lewis, J., 2002. Chapter 6: How cells read the genome: From DNA to protein. *In*: *Molecular Biology of the Cell*. Garland Science, 299–374.

Anderson, J. M., 2001. Biological Responses to Materials. *Annu. Rev. Mater. Res.*, 31, 81–110.

Anderson, J. M., 2004. *Biomaterial Science- An Introduction to Materials in Medicine: Chapter 4 Host Reactions to Biomaterials and Their Evaluation*. 2nd ed.

Anderson, J. M., Rodriguez, A., and Chang, D. T., 2008. Foreign body reaction to biomaterials. *Seminars in Immunology*, 20 (2), 86–100.

Ang, K., Tamborlane, W. S., and Weinzimer, S. A., 2015. Combining glucose monitoring and insulin delivery into a single device: current progress and ongoing challenges of the artificial pancreas. *Expert Opin Drug Deliv.*, 12 (10), 1579–1582.

Avraamides, C. J., Garmy-susini, B., and Varner, J. A., 2008. Integrins in angiogenesis and lymphangiogenesis. *Nat Rev Cancer*, 8 (8), 604–617.

Ben-Yosef, Y., Lahat, N., Shapiro, S., Bitterman, H., and Miller, A., 2002. Regulation of Endothelial Matrix Metalloproteinase-2 by Hypoxia/Reoxygenation. *Circ Res*, 90, 784–791.

Ben-Yosef, Y., Miller, A., Shapiro, S., Lahat, N., Miller, A., and Shapiro, S., 2005. Hypoxia of endothelial cells leads to MMP-2-dependent survival and death. *Am J Physio Cell Physiol*, 289, 1321–1331.

Border, W. A. and Ruoslahti, E., 1992. Transforming growth factor-beta in disease: the dark side of tissue repair. *Journal of Clinical Investigation* [online], 90 (1), 1–7. Available from: http://www.jci.org/articles/view/115821.

Carmeliet, P., 2005. VEGF as a Key Mediator of Angiogenesis in Cancer. *Oncology*, 69 (suppl 3), 4–10.

Chiang, J. L., Kirkman, M. S., Laffel, L. M. B., and Peters, A. L., 2014. Type 1 diabetes through the life span: A position statement of the American Diabetes Association. *Diabetes Care*, 37 (7), 2034–2054.

Cobelli, C., Renard, E., and Kovatchev, B., 2011. Artificial pancreas: Past, present, future. *Diabetes*, 60 (11), 2672–2682.

Colditz, G. A., Braun, L. T., and McCulloch, D. K., 2005. Diabetic Ketoacidosis. *Complications of Diabetes Module* [online]. Available from: https://www.google.co.id/url?sa=t&rct=j&q=&esrc=s&source=web&cd=1&cad=rja&uact=8&ved=0ahUKEwjDidvYpI3TAhVKso8KHWxODBQQFggbMAA&url=http%3A%2F%2Fvirtuallabs.stanford.edu%2Fdiabetes%2FDiabetesModuleTextAll.pdf&usg=AFQjCNFjJCjpVaeqd-zfeX9Qk876aGIPsA.

Dana, N., Fathallah, D. M., and Arnaout, M. A., 1991. Expression of a soluble and functional form of the human beta2 integrin CD11b/CD18. *Proc. Natl. Acad. Sci. USA*, 88, 3106–3110.

Daneman, D., 2006. Type 1 diabetes. *Lancet* [online], 367, 847–858. Available from: http://www.ncbi.nlm.nih.gov/entrez/query.fcgi?cmd=Retrieve&db=PubMed&dopt=Citation&list_uids=11526380.

Delisser, H. M., Newman, P. J., and Albelda, S. M., 1994. Review: Molecular and functional aspects of PECAM-1/CD31. *Immunol Today*, 15 (10), 490–495.

Diabetes.co.uk, 2017. *Artificial Pancreas* [online]. Available from: http://www.diabetes.co.uk/artificial-pancreas.html [Accessed 2 Jul 2017].

Dixelius, J., Olsson, A. K., Thulin, Å., Lee, C., Johansson, I., and Claesson-Welsh, L., 2006. Minimal active domain and mechanism of action of the angiogenesis inhibitor histidine-rich glycoprotein. *Cancer Research*, 66 (4), 2089–2097.

Facchinetti, A., Sparacino, G., Guerra, S., Luijf, Y. M., De Vries, J. H., Mader, J. K., Ellmerer, M., Benesch, C., Heinemann, L., Bruttomesso, D., Avogaro, A., and Cobelli, C., 2013. Real-time improvement of continuous glucose monitoring accuracy: The smart sensor concept. *Diabetes Care*, 36 (4), 793–800.

Feng, Y., Chen, X., and Zhang, X., 2016. Roles of PECAM-1 in cell function and disease progression. *Eur Rev Med Pharmacol Sci*, 20 (19), 4082–4088.

Fossati-Jimack, L., Ling, G. S., Cortini, A., Szajna, M., Malik, T. H., Mcdonald, J. U., Pickering, M. C., Cook, H. T., Taylor, P. R., and Botto, M., 2013. Phagocytosis Is the Main CR3-Mediated Function Affected by the Lupus-Associated Variant of CD11b in Human Myeloid Cells. *PloS one*, 8 (2), e57082.

Gifford, R., 2013. Continuous glucose monitoring: 40 years, what we've learned and what's next. *ChemPhysChem*, 14 (10), 2032–2044.

Goerges, A. L. and Nugent, M. A., 2004. pH Regulates Vascular Endothelial Growth Factor Binding to Fibronectin, 279 (3), 2307–2315.

Gutteridge, J. M. C., 1994. Biological origin of free radicals, and mechanisms of antioxidant protection. *Chem Biol Interact.*, 91 (2–3), 133–140.

Guzy, R. D. and Schumacker, P. T., 2006. Oxygen sensing by mitochondria at complex III : the paradox of increased reactive oxygen species during hypoxia, 807–819.

Hajnsek, M., Nacht, B., Sax, S., List, E. J. W., Klimant, I., and Sinner, F., 2014. The single-port concept: combining optical glucose measurement with insulin infusion. *Acta Diabetologica*, 51 (5), 883–886.

Hausman, G. J. and Richardson, R. L., 2004. Adipose tissue angiogenesis, 925–934.

Hauzenberger, J. R., Hipszer, B. R., Loeum, C., McCue, P. A., DeStefano, M., Torjman, M. C., Kaner, M. T., Dinesen, A. R., Chervoneva, I., Pieber, T. R., and Joseph, J. I., 2017. Detailed Analysis of Insulin Absorption Variability and the Tissue Response to Continuous Subcutaneous Insulin Infusion Catheter Implantation in Swine. *Diabetes Technology & Therapeutics* [online], 19 (11), 641–650. Available from: http://online.liebertpub.com/doi/10.1089/dia.2017.0175.

Hauzenberger, J. R., Münzker, J., Kotzbeck, P., Asslaber, M., Bubalo, V., Joseph, J. I., and Pieber, T. R., 2018. Systematic in vivo evaluation of the time-dependent inflammatory response to steel and Teflon insulin infusion catheters. *Scientific Reports* [online], 8 (1), 1132. Available from: http://www.nature.com/articles/s41598-017-18790-0.

He, Q., Gao, Z., Yin, J., Zhang, J., Yun, Z., and Ye, J., 2011. Regulation of HIF-1 activity in adipose tissue by obesity-associated factors: adipogenesis, insulin, and hypoxia. *AJP: Endocrinology and Metabolism* [online], 300 (5), E877–E885. Available from: http://ajpendo.physiology.org/cgi/doi/10.1152/ajpendo.00626.2010.

Heinemann, L., 2016. Insulin Infusion Sets: A Critical Reappraisal. *Diabetes Technology & Therapeutics* [online], 18 (5), 327–333. Available from: http://online.liebertpub.com/doi/10.1089/dia.2016.0013.

Heinemann, L., Walsh, J., and Roberts, R., 2014. We need more research and better designs for insulin infusion sets. *Journal of Diabetes Science and Technology*, 8 (2), 199–202.

Higgins, D. F., Kimura, K., Bernhardt, W. M., Shrimanker, N., Akai, Y., Hohenstein, B., Saito, Y., Johnson, R. S., Kretzler, M., Cohen, C. D., Eckardt, K. U., Iwano, M., and Haase, V. H., 2007. Hypoxia promotes fibrogenesis in vivo via HIF-1 stimulation of epithelial-to-mesenchymal transition. *Journal of Clinical Investigation*, 117 (12), 3810–3820.

Holzapfel, B. and Wickert, L., 2007. Die quantitative Real-Time-PCR (qRT-PCR). Methoden und Anwendungsgebiete. *Biologie in unserer Zeit* [online], 37 (2), 120–126. Available from: http://doi.wiley.com/10.1002/biuz.200610332.

Ignotz, R. a, Endo, T., and Massagué, J., 1987. Regulation of fibronectin and type I collagen mRNA levels by transforming growth factor-beta. *The Journal of biological chemistry* [online], 262 (14), 6443–6. Available from: http://www.ncbi.nlm.nih.gov/pubmed/3471760.

International Union of Food Science and Technology and (IUFoST), 2013. *The World of Food Science* [online]. Available from: http://worldfoodscience.com/article/surveillance-genetically-modified-plants-food-feed-and-seed [Accessed 19 Oct 2017].

Joanneum Research Forschungsgesellschaft mbH, (JR), 2012. *SPIDIMAN project* [online]. SPIDIMAN. Available from: http://www.spidiman.eu/ [Accessed 27 Jan 2018].

Jozefczuk, J. and Adjaye, J., 2011. *Quantitative real-time PCR-based analysis of gene expression* [online]. 1st ed. Methods in Enzymology. Elsevier Inc. Available from: http://dx.doi.org/10.1016/B978-0-12-385118-5.00006-2.

Kominsky, D. J., Campbell, E. L., and Colgan, S. P., 2010. Metabolic Shifts in Immunity and Inflammation. *J Immunol*, 184 (8), 4062–4068.

Krzewska, A. and Ben-Skowronek, I., 2016. Effect of Associated Autoimmune Diseases on Type 1 Diabetes Mellitus Incidence and Metabolic Control in Children and Adolescents. *BioMed Research International*, 2016.

Lebre, F., Sridharan, R., Sawkins, M. J., Kelly, D. J., O'Brien, F. J., and Lavelle, E. C., 2017. The shape and size of hydroxyapatite particles dictate inflammatory responses following implantation. *Scientific Reports*, 7 (1), 2922.

Lee, J.-W., Bae, S.-H., Jeong, J.-W., Kim, S.-H., and Kim, K.-W., 2004. Hypoxia-inducible factor (HIF-1)alpha: its protein stability and biological functions. *Experimental & molecular medicine*, 36 (1), 1–12.

Lenselink, E. A., 2013. Role of fibronectin in normal wound healing, 1–4.

Liekens, S., De Clercq, E., and Neyts, J., 2001. Angiogenesis: Regulators and clinical applications. *Biochemical Pharmacology*, 61 (3), 253–270.

Lindpointner, S., Korsatko, S., Gerd Köhler, H. K., Schaller, R., Kaidar, R., Yodfat, O., Schaupp, L., Ellmerer, M., Pieber, T. R., and Regittnig, W., 2010. Administration for the Measurement of Glucose in Patients With Type 1 Diabetes. *Diabetes Care*, 33, 595–601.

Lindpointner, S., Korsatko, S., and Köhler, G., 2010. Glucose levels at the site of subcutaneous insulin administration and their relationship to plasma levels. *Diabetes Care* [online], 33, 833–838. Available from: http://care.diabetesjournals.org/content/33/4/833.short.

Matlaga, B. F., Yasenchak, L. P., and Salthouse, T. N., 1976. Tissue response to implanted polymers: The significance of sample shape. *Journal of Biomedical Materials Research*, 10 (3), 391–397.

Meyer, W., Schwarz, R., and Neurand, K., 1978. The skin of domestic mamals as a model for the human skin, with special reference to the domestic pig. *Current problems in dermatology*, 7, 39–52.

Minutti, C. M., Knipper, J. A., Allen, J. E., and Zaiss, D. M. W., 2017. Tissue-specific contribution of macrophages to wound healing. *Seminars in Cell and Developmental Biology* [online], 61, 3–11. Available from: http://dx.doi.org/10.1016/j.semcdb.2016.08.006.

Morais, J. M., Papadimitrakopoulos, F., and Burgess, D. J., 2010. Biomaterials/Tissue Interactions: Possible Solutions to Overcome Foreign Body Response. *The AAPS Journal* [online], 12 (2), 188–196. Available from: http://www.springerlink.com/index/10.1208/s12248-010-9175-3.

Murphy, J. F. and Fitzgerald, D. J., 2001. Vascular endothelial growth factor induces cyclooxygenase-dependent proliferation of endothelial cells via the VEGF-2 receptor. *FASEB journal : official publication of the Federation of American Societies for Experimental Biology*, 15 (9), 1667–1669.

Neels, J. G., Thinnes, T., and Loskutoff, D. J., 2004. Angiogenesis in an in vivo model of adipose tissue development. *FASEB J*, 18 (9), 983–5.

Newman, P. J., 1994. The Role of PECAM-1 in Vascular Cell Biologya. *Annals of the New York Academy of Sciences* [online], 714 (1), 165–174. Available from: http://dx.doi.org/10.1111/j.1749-6632.1994.tb12041.x.

Newman, P. J. and Newman, D. K., 2003. Signal Transduction Pathways Mediated by PECAM-1 New Roles for an Old Molecule in Platelet and Vascular Cell Biology. *Arterioscler Thromb Vasc Biol*, 23, 953–964.

Nygard, A., Jørgensen, C. B., Cirera, S., and Fredholm, M., 2007. Selection of reference genes for gene expression studies in pig tissues using SYBR green qPCR, 6, 1–6.

Österreichische Diabetes Gesellschaft, 2017. *FACE DIABETES – Zahlen und Fakten zu Diabetes mellitus* [online]. Available from: http://www.facediabetes.at/zahlen-und-fakten.html [Accessed 18 Apr 2017].

Parekh, T., Saxena, B., Reibman, J., Cronstein, B. N., and Gold, L. I., 1994. Neutrophil chemotaxis in response to TGF-beta isoforms (TGF-beta 1, TGF-beta 2, TGF-beta 3) is mediated by fibronectin 20. *J.Immunol.*, 152 (0022–1767 (Print)), 2456–2466.

Patel, P. J., Benasi, K., Ferrari, G., Evans, M. G., Shanmugham, S., Wilson, D. M., and Buckingham, B. A., 2014. Randomized Trial of Infusion Set Function: Steel Versus Teflon. *Diabetes Technology & Therapeutics* [online], 16 (1), 15–19. Available from: http://online.liebertpub.com/doi/abs/10.1089/dia.2013.0119.

Phillips, A., 2016. Supporting patients with type 1 diabetes. *British Journal of Nursing* [online], 25 (6), 330–334. Available from: http://www.magonlinelibrary.com/doi/10.12968/bjon.2016.25.6.330.

Pickup, J. and Keen, H., 2002. Continuous Subcutaneous Insulin Infusion at 25 Years. *Diabetes Care*, 25, 593–598.

Pittman, R. N., 2013. *Oxygen Transport in the Microcirculation and Its Regulation*. Microcirculation.

Postlethwaite, A. E., Keski-Oja, J., Moses, H. L., and Kang, A. H., 1987. Stimulation of the chemotactic migration of human fibroblasts by transforming growth factor beta. *The Journal of experimental medicine* [online], 165 (1), 251–6. Available from: http://www.pubmedcentral.nih.gov/articlerender.fcgi?artid=2188256&tool=pmcentrez&rendertype=abstract.

Ratner, B. D. and Bryant, S. J., 2004. Biomaterials: Where We Have Been and Where We Are Going. *Annual Review of Biomedical Engineering* [online], 6 (1), 41–75. Available from: http://www.annualreviews.org/doi/10.1146/annurev.bioeng.6.040803.140027.

Regittnig, W., Lindpointner, S., Korsatko, S., Tutkur, D., Bodenlenz, M., and Pieber, T. R., 2013. Periodic extraction of interstitial fluid from the site of subcutaneous insulin infusion for the measurement of glucose: a novel single-port technique for the treatment of type 1 diabetes patients. *Diabetes technology & therapeutics* [online], 15 (1), 50–9. Available from: http://www.ncbi.nlm.nih.gov/pubmed/23126579%5Cnhttp://www.pubmedcentral.nih.gov/articlerender.fcgi?artid=PMC3540899.

Robert, N., 2013. The Artificial Pancreas: A Race To The Finish. *MedTech Insight* [online], 1–8. Available from: http://cdn.jdrf.org/wp-content/uploads/2013/11/MTI1310_Artificial-Pancreas_2013700119.pdf.

Roberts, A. B., Sporn, M. B., Assoian, R. K., Smith, J. M., Roche, N. S., Wakefield, L. M., Heine, U. I., Liotta, L. A., Falanga, V., and Kehrl, J. H., 1986. Transforming growth factor type beta: rapid induction of fibrosis and angiogenesis in vivo and stimulation of collagen formation in vitro. *Proceedings of the National Academy of Sciences* [online], 83 (12), 4167–4171. Available from: http://www.pnas.org/cgi/doi/10.1073/pnas.83.12.4167.

Rodbard, D., 2016. Continuous Glucose Monitoring: A Review of Successes, Challenges, and Opportunities. *Diabetes Technology & Therapeutics* [online], 18 (S2), S2-3-S2-13. Available from: http://online.liebertpub.com/doi/10.1089/dia.2015.0417.

Rumpler, M., Mader, J. K., Fischer, J. P., Thar, R., Granger, J. M., Deliane, F., Klimant, I., Aberer, F., Sinner, F., Pieber, T. R., and Hajnsek, M., 2017. First application of a transcutaneous optical single-port glucose monitoring device in patients with type 1 diabetes mellitus. *Biosensors and Bioelectronics*, 88, 240–248.

SA Biosciences, 2008. Real-Time PCR for Systems Biology : A Review on Real-time PCR-related Technologies & their applications in the Post-Genomic Era. *Pathways*, (8), 14–16.

Sariahmetoglu, M., Crawford, B. D., Leon, H., Sawicka, J., Li, L., Ballermann, B. J., Holmes, C., Berthiaume, L. G., Holt, A., Sawicki, G., Schulz, R., and Regulation, R., 2017. Regulation of matrix metalloproteinase-2 (MMP-2) activity by phosphorylation, 21 (10), 2486–2495.

Schoen, F. J., 2004. *Biomaterial Science - An Introduction to Materials in Medicine: Chapter 4 Host Reactions to Biomaterials and Their Evaluation* [online]. 2nd ed. Elsevier Academic Press. Available from: http://ilkerpolatoglu.cbu.edu.tr/docs/Introduction to Materials.pdf.

Seaton, M., Hocking, A., and Gibran, N. S., 2015. Porcine models of cutaneous wound healing. *ILAR Journal*, 56 (1), 127–138.

Shalitin, S. and Phillip, M., 2007. The role of new technologies in treating children and adolescents with type 1 diabetes mellitus. *Pediatric Diabetes* [online], 8 (s6), 72–79. Available from: http://doi.wiley.com/10.1111/j.1399-5448.2007.00279.x.

Sides, C. R. and Stenken, J. A., 2014. Microdialysis Sampling Techniques Applied to Studies of the Foreign Body Reaction. *Eur J Pharm Sci*, 16 (57), 74–86.

Sikes, K. A. and Weyman, K., 2017. *Diabetes and the Use of Insulin Pumps* [online]. Endocrinology Metabolism. Available from: https://www.clinicaladvisor.com/endocrinology-metabolism/diabetes-and-the-use-of-insulin-pumps/article/595843/ [Accessed 17 Aug 2017].

Silbernagl, S. and Lang, F., 2013. Akute Auswirkungen des Insulinmangels (Diabetes mellitus). *In*: *Taschenatlas der Pathophysiologie* [online]. Georg Thieme Verlag, 314–315. Available from: https://books.google.at/books?id=CYxrAAAAQBAJ&pg=PA314&dq=taschenatlas+pathophysiologie+insulinmangel&hl=de&sa=X&ved=0ahUKEwih0viavMDUAhVJaxQKHZ0oADgQ6AEIJjAA#v=onepage&q=taschenatlas pathophysiologie insulinmangel&f=false.

Sino Biological Inc., 2016. *Real-time PCR Service: Gene Expression Analysis by qPCR* [online]. Available from: http://www.sinobiological.com/real-time-pcr-service-gene-expression-analysis-by-qpcr-cro-service.html [Accessed 19 Oct 2017].

Solovjov, D. A., Pluskota, E., and Plow, E. F., 2005. Distinct Roles for the α and β Subunits in the Functions of Integrin αMβ2. *Journal of Biological Chemistry*, 280 (2), 1336–1345.

Soltesz, G., Patterson, C. C., and Dahlquist, G., 2007. Worldwide childhood type 1 diabetes incidence--what can we learn from epidemiology? *Pediatric diabetes*, 8 Suppl 6, 6–14.

Sullivan, T. P., Eaglstein, W. H., Davis, S. C., and Mertz, P., 2001. The pig as a model for human wound healing. *Wound repair and regeneration* [online], 9 (2), 66–76. Available from: http://www.ncbi.nlm.nih.gov/pubmed/11350644%5Cnhttp://doi.wiley.com/10.1046/j.1524-475x.2001.00066.x.

Thabit, H. and Hovorka, R., 2016. Coming of age: the artificial pancreas for type 1 diabetes. *Diabetologia*, 59 (9), 1795–1805.

Todd, J. A., 2010. Etiology of Type 1 Diabetes. *Immunity* [online], 32 (4), 457–467. Available from: http://dx.doi.org/10.1016/j.immuni.2010.04.001.

Tonnesen, M. G., Feng, X., and Clark, R. A. F., 2000. Angiogenesis in Wound Healing. *Journal of Investigative Dermatology Symposium Proceedings* [online], 5 (1), 40–46. Available from: http://dx.doi.org/10.1046/j.1087-0024.2000.00014.x.

Trachtenbarg, D. E., 2005. Diabetic ketoacidosis. *American Family Physician*, 71 (9), 1705–1714.

Tschaikner, M., Powell, K., Jungklaus, M., Fritz, M., Ellmerer, M., Hovorka, R., Lane, S., Pieber, T. R., and Regittnig, W., 2015. Miniaturisierung der künstlichen Bauchspeicheldrüse durch Zusammenlegung von Insulingabe und Glukosemessung im subkutanen Fettgewebe. *Wiener Klinische Wochenschrift*, 127, 146–147.

Voet, D., Voet, J. G., and Pratt, C. W., 2002. Störungen im Energiestoffwechsel. *In*: Beck-Sickinger, A. G. and Hahn, U., eds. *Lehrbuch der Biochemie*. Leipzig: Wiley-VCH, 719–725.

Wang, H. C. and Lee, A. R., 2015. Recent developments in blood glucose sensors. *Journal of Food and Drug Analysis* [online], 23 (2), 191–200. Available from: http://dx.doi.org/10.1016/j.jfda.2014.12.001.

Wang, J. F., Olson, M. E., Reno, C. R., Wright, J. B., and Hart, D. A., 2001. The pig as a model for excisional skin wound healing: characterization of the molecular and cellular biology, and bacteriology of the healing process. *Comp Med* [online], 51 (4), 341–348. Available from: https://www.ncbi.nlm.nih.gov/pubmed/11924793.

Weissberg-Benchell, J., Antisdel-Lomaglio, J., and Seshadri, R., 2003. Insulin Pump Therapy. *Diabetes Care*, 26 (4), 1079–1087.

Werner, S. and Grose, R., 2003. Regulation of wound healing by growth factors and cytokines. *Physiological reviews*, 83 (3), 835–870.

Wijelath, E. S., Murray, J., Rahman, S., Patel, Y., Ishida, A., Strand, K., Aziz, S., Cardona, C., Hammond, W. P., Savidge, G. F., Rafii, S., and Sobel, M., 2002. Novel Vascular Endothelial Growth Factor Binding Domains of Fibronectin Enhance Vascular Endothelial Growth Factor Biological Activity.

Wiseman, D. M., Polverini, P. J., Kamp, D. W., and Leibovich, S. J., 1988. TGF-b is chemotactic for human monocytes and induces their expression of angiogenic activity. *Biochemical and Biophysical Research Communications*, 157 (2), 793–800.

Zeitouni, N. E., Chotikatum, S., Köckritz-blickwede, M. Von, and Naim, H. Y., 2016. The impact of hypoxia on intestinal epithelial cell functions : consequences for invasion by bacterial pathogens. *Molecular and Cellular Pediatrics* [online]. Available from: http://dx.doi.org/10.1186/s40348-016-0041-y.

10. Appendix

Table 2: Oligo names and sequences used for genes in swine for SYBR Green qPCR.

Name	Sequence	Comment
TGFb_fw	AAAACAGGAAGGCAGTGTGG	Gene of interest
TGFb_rv	TAGGCTGCTTTCTTGGCTTC	Gene of interest
VEG_-fw	GAGGCAAGAAAATCCCTGTG	Gene of interest
VEGF_rv	GAGGCAAGAAAATCCCTGTG	Gene of interest
HIF1α_fw	TGCTCATCAGTTGCCACTTC	Gene of interest
HIF1α_rv	TCCTCACACGCAAATAGCTG	Gene of interest
CD31_fw	AAAGGAGAACAAGCCCTTCC	Gene of interest
CD31_rv	TGGAGGCCAGGCAATAATAC	Gene of interest
MMP2_fw	ATTGCAAGTTCCCCTTCTCC	Gene of interest
MMP2_rv	ACTTGCCATCCTTGTCGAAG	Gene of interest
CD11b_fw	TCACGGACGGAGAAAAGTTC	Gene of interest
CD11b_rv	CGATGACATAGCGAATGACG	Gene of interest
FN_fw	TTATCAGGGCTGGATGATGG	Gene of interest
FN_rv	TTCTGGTGTCCTGATCGTTG	Gene of interest
YWHAZ_fw	CACAGCAAGCATACCAGGAA	Reference gene
YWHAZ_rv	GTTCAGCAATGGCTTCATCA	Reference gene
RPL4_fw	AGGAGGCTGTTCTGCTTCTG	Reference gene
RPL4_rv	TCCAGGGATGTTTCTGAAGG	Reference gene